JOURNAL OF GEOPHYSICAL RESEARCH, VOL. 100, NO. B7, PAGES 9761–9788, JUNE 10, 1995

Seismic velocity structure and composition of the continental crust: A global view

Nikolas I. Christensen

Department of Earth and Atmospheric Sciences, Purdue University, West Lafayette, Indiana

Walter D. Mooney

U.S. Geological Survey, Menlo Park, California

Abstract. Seismic techniques provide the highest-resolution measurements of the structure of the crust and have been conducted on a worldwide basis. We summarize the structure of the continental crust based on the results of seismic refraction profiles and infer crustal composition as a function of depth by comparing these results with high-pressure laboratory measurements of seismic velocity for a wide range of rocks that are commonly found in the crust. The thickness and velocity structure of the crust are well correlated with tectonic province, with extended crust showing an average thickness of 30.5 km and orogens an average of 46.3 km. Shields and platforms have an average crustal thickness nearly equal to the global average. We have corrected for the nonuniform geographical distribution of seismic refraction profiles by estimating the global area of each major crustal type. The weighted average crustal thickness based on these values is 41.1 km. This value is 10% to 20% greater than previous estimates which underrepresented shields, platforms, and orogens. The average compressional wave velocity of the crust is 6.45 km/s, and the average velocity of the uppermost mantle (*Pn* velocity) is 8.09 km/s. We summarize the velocity structure of the crust at 5-km depth intervals, both in the form of histograms and as an average velocity-depth curve, and compare these determinations with new measurements of compressional wave velocities and densities of over 3000 igneous and metamorphic rock cores made to confining pressures of 1 GPa. On the basis of petrographic studies and chemical analyses, the rocks have been classified into 29 groups. Average velocities, densities, and standard deviations are presented for each group at 5-km depth intervals to crustal depths of 50 km along three different geotherms. This allows us to develop a model for the composition of the continental crust. Velocities in the upper continental crust are matched by velocities of a large number of lithologies, including many low-grade metamorphic rocks and relatively silicic gneisses of amphibolite facies grade. In midcrustal regions, velocity gradients appear to originate from an increase in metamorphic grade, as well as a decrease in silica content. Tonalitic gneiss, granitic gneiss, and amphibolite are abundant midcrustal lithologies. Anisotropy due to preferred mineral orientation is likely to be significant in upper and midcrustal regions. The bulk of the lower continental crust is chemically equivalent to gabbro, with velocities in agreement with laboratory measurements of mafic granulite. Garnet becomes increasingly abundant with depth, and mafic garnet granulite is the dominant rock type immediately above the Mohorovicic discontinuity. Average compressional wave velocities of common crustal rock types show excellent correlations with density. The mean crustal density calculated from our model is 2830 kg/m^3, and the average SiO_2 content is 61.8%.

Introduction

Knowledge of the structure and petrology of the continental crust is of fundamental importance in understanding crustal generation and evolution. The last two decades have witnessed a remarkable increase in seismic measurements of crustal structure. In the past, seismic refraction models of crustal structure were usually presented in terms of rather simple layer models. Recently, however, layered crustal models have been generally discarded in favor of more geologically reasonable gradient models, often with lateral variabilities, which emphasize local structural complexities. Seismic reflectivity also varies widely in different geologic provinces, providing additional support for the existence of crustal heterogeneity. These new seismic images of the continental crust are consistent with a complex origin involving multiple episodes of accretion, deformation, metamorphism, plutonism, and volcanism.

Even though a variety of geologic and geophysical studies have provided an important framework for our understanding of the continental crust, serious deficiencies remain in our knowledge of the geological processes that create and rework continental crust. Only when sufficiently detailed information on the distribution of rock types with depth, as well as their lateral variability, is obtained, will an understanding of the geologic processes that form continental crust be possible.

Paper number 95JB00259.
0148-0227/95/95JB-00259$05.00

This paper summarizes the seismic structure of the continental crust on the basis of a new worldwide data compilation. The term continental crust, as used here, includes all land masses above sea level, with the exception of oceanic volcanic plateaus, such as Iceland and Hawaii. Continental margins are not included, since these areas usually have a seismic structure that is intermediate between oceanic crust and continental crust. In order to interpret seismic observations in terms of crustal petrology and chemistry, we present velocities of compressional waves as functions of depth and temperature for major rock types believed to be significant constituents of the continental crust and upper mantle. This compilation of laboratory velocity data for a wide variety of continental igneous and metamorphic rock types provides a basis for the new interpretation of crustal composition. In this paper, we do not attempt to present a survey of all previous work relating to the composition and structure of the continental crust but instead focus on the integration of the compilations. For comprehensive discussions of previous ideas on crustal composition, the reader is referred to review articles by *Kay and Kay* [1981], *Fountain and Christensen* [1989], *Percival et al.* [1992], *Holbrook et al.* [1992], *Rudnick* [1992], and *Downs* [1993].

Seismic Refraction Observations

A total of 560 determinations of the velocity-depth structure of the crust have been compiled in this study (Figure 1). Every effort has been made to include all global seismic refraction measurements of the continental crust which we have determined to be reliable. Continental margins have not been included, but measurements in inland seas and lakes, such as Hudson's Bay, the Great Lakes of North America, and Lake Baikal, have been included. These data were compiled from the published literature and from a limited number of unpublished reports. The published literature covers the years 1950-1993 and includes journal articles, monographs, and special publications such as meeting proceedings, governmental open file reports, and annual reports of research institutions. Unpublished literature consists primarily of high-quality technical reports of recent field measurements that have been issued prior to journal publication. Table 1 lists the previous compilations of seismic refraction data that have been included in this compilation. It is evident from Figure 1 that the geographical distribution of seismic refraction profiles is uneven, with many profiles in central North America, western Europe, Eurasia, and

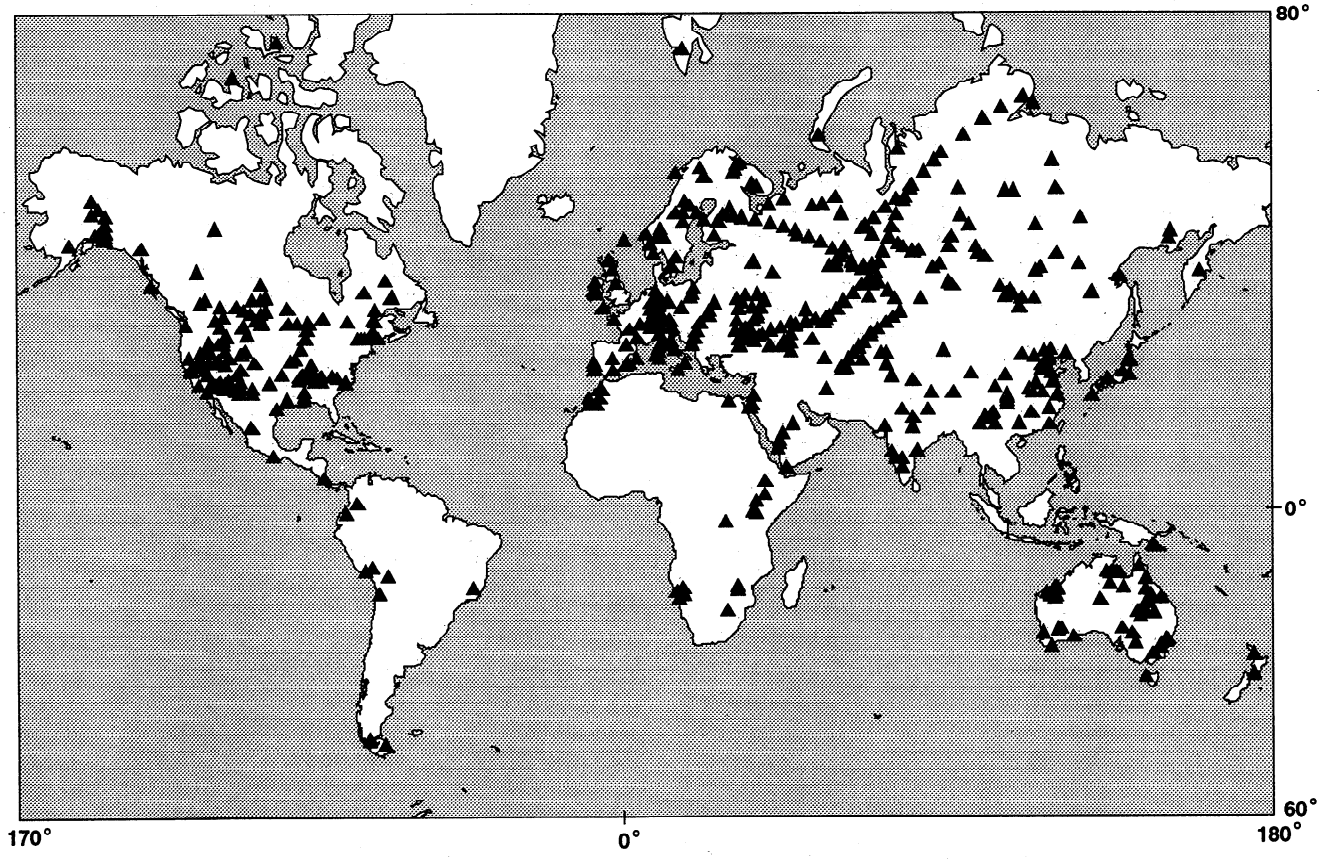

Figure 1. Locations (solid triangles) of 560 individual velocity-depth functions compiled for this study. Only the results of seismic refraction/wide-angle reflection profiles have been used. Individual triangles are located at the midpoint of individual crustal-scale profiles. A single determination in Antarctica is not shown. Lines of triangles at uniform spacing are indicative of long-range seismic refraction profiles with detailed crustal information. No effort has been made to average independent neighboring determinations into a single measurement; rather this averaging has been accomplished through the use of histograms of large numbers of measurements. Principal data sources are listed in Table 1. Data selection and interpretation uncertainties are discussed in the text.

Table 1. Seismic Refraction Data Compilations

Reference	Number of Profiles	Region Covered
Tuve et al. [1954]	15	North America
Press [1966]	30	global
James and Steinhart [1966]	30	North America
McConnell et al. [1966]	100	global
Warren and Healy [1974]	40	North America
Giese et al. [1976]	80	Europe
Christensen [1982]	278	global
Allenby and Schnetzler [1983]	200	North America
Soller et al. [1982]	297	global
Prodehl [1984]	200	global
Meissner [1986]	150	global
Meissner et al. [1987]	100	Europe
Braile et al. [1989]	200	North America
Mooney and Braile [1989]	220	North America
Collins [1988]	50	Australia
Mechie and Prodehl [1988]	20	Afr-Arabia
Beloussov et al. [1991]	120	former USSR
Holbrook et al. [1992]	90	global
Kaila and Krishna [1992]	25	India
GEON Center [1994]	200	former USSR
Li and Mooney [1995]	25	China
Total number of profiles compiled here	560	global

Australia. There is an underrepresentation of data from Africa, South America, northern Canada, Antarctica, and Greenland. Despite these gaps in geographical coverage, the available data include more than adequate coverage to allow us to accurately characterize continental crust.

Reliability and Precision

The reliability of published crustal velocity models is critical to the usefulness of the compilation used here, especially as no new crustal models have been recalculated for this study. Rather, published interpretations have been evaluated for reliability.

A variety of methods have been used to interpret the seismic refraction data used in this compilation [cf. *Mooney*, 1989]. By far the most common method is the interpretation of seismic traveltimes (but not amplitudes) using either one- or two-dimensional modeling methods. Since about 1980, most interpretations have involved the application of raytracing to compare the traveltimes through a two-dimensional (2-D) velocity model with observed traveltimes. Prior to 1980, most crustal models were developed in terms of either plane-dipping layers or by interpolating a set of 1-D models into a 2-D model. In the former Soviet Union and India, very dense data sets were recorded, and complex 2-D models could be constructed from well-recorded wide-angle reflections that imaged major crustal velocity discontinuities.

The modeling of seismic amplitudes, in addition to travel times, became routinely possible with the development of efficient computer codes for the calculation of amplitudes in one- and two-dimensional media. For 1-D media, the most commonly used method is the reflectivity method of *Fuchs and Muller* [1971], which can provide the complete seismic response of an elastic media, including seismic velocity gradients and low velocity zones. Inverse methods, which provide seismic velocity models based on the direct inversion of the data, have been developed in the last 10 years but have been applied in less than 5% of the results compiled here.

Data quality control is an important consideration in any compilation of global geophysical data. In the present case, these seismic profiles have been collected over a period of 40 years by more than 100 separate investigators. Therefore careful guidelines have been adopted. First, where coincident data sets are available, a selection has been made of the higher-quality data with a more modern interpretation. Second, where only one data set is available, an assessment has been made of the quality of the published interpretation prior to inclusion in this compilation. Major considerations included (1) signal-to-noise levels and spatial density of the data; (2) clarity of secondary phases used to interpret crustal layering and Moho depth; and (3) use of appropriate methods to compare theoretical and observed travel times and, in many cases, seismic amplitudes. However, for some older publications these guidelines are difficult to apply as these papers do not include many examples of the recorded data and the method of data interpretation is not fully described. In these cases, which constitute only 10% of the data compiled here, a critical assessment of the data reliability has been made based on the written description of the data acquisition and interpretation methods.

In the seismic refraction method, apparent seismic velocities are directly measured, while the depths of refracting horizons are successively calculated from the uppermost layer to the deepest layer measured. Thus seismic velocity determinations generally have lower percent errors than depth determinations. For the seismic profile data compiled here, seismic velocities are accurate to 3%, or about ± 0.2 km/s. Velocities are 2 or 3 times less accurate for the few unreversed profiles that we have included for geographical completeness. The 3% velocity uncertainty is conservative and is discussed by *Mooney* [1989] and *Holbrook et al.* [1992]. It is based on such factors as the accuracy of seismic arrival-time determinations, chronometer corrections, field surveying uncertainties, typical seismograph and shot point spacings, and effects of lateral variations in near-surface low-velocity anomalies, especially sedimentary basins. All boundary depths (including the Moho) are accurate to about 10% of the depth. Thus a reported crustal thickness of 40 km typically has an uncertainty of ± 4 km.

Crustal Thickness, Average Crustal Velocity, and *Pn* Velocity

Perhaps the most basic parameter regarding the continental crust is total thickness (surface to Mohorovicic discontinuity). Because all previous estimates of average crustal thickness have been based on the simple average value from reported measurements, we have also calculated this unweighted average. In addition, we have calculated a more accurate average that is weighted by the percent area of crust that consists of five basic crustal types described below. This weighted average corrects for biases that result from the numerous measurements that are available for the thin extended crust of western Europe and the western North America, in contrast to the sparse measurements available for the thicker crust of Africa, South America, Antarctica, and Greenland.

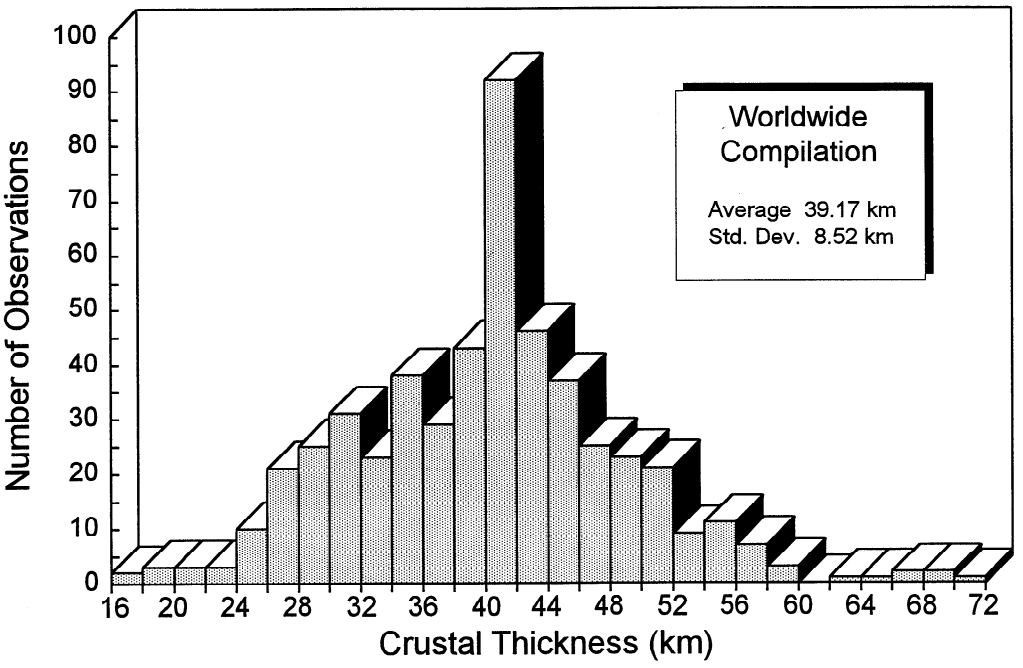

Figure 2. Histogram of crustal thickness. Locations of data are shown in Figure 1. The thickness shown in the box is the average of 560 measurements. The weighted average crustal thickness, based on estimated proportions of tectonic provinces by area, is 41.0 km ± 6.2 km.

Our worldwide compilation shows that the mean crustal thickness expressed as the unweighted average of reliable observations is 39.2 km, with a standard deviation of 8.5 km (Figure 2). The thinnest reported continental crust is 16 km (Afar Triangle, Ethiopia, recently transitional from oceanic) and the thickest (as determined from seismic refraction data) is 72 km (Tibetan Plateau, China). Recalling the estimated 10% error in depth determinations, the continental crust can be said to vary in thickness between 14 and 80 km. However, more that 95% of all measurements fall within two standard deviations, between 22 km and 57 km.

Our estimate of mean crustal thickness is higher than many previous estimates (Table 2). This can be attributed to the inclusion of a substantial amount of newly available data from the former Soviet Union which includes 40-50 km thick platform and shield crust.

Average crustal velocity (Figure 3) is a parameter that is well determined from seismic refraction data. Our data provides a value of average crustal velocity of 6.45 km/s, with a standard deviation of 0.23 km/s. This unweighted value is higher than some earlier estimates [e.g., *Smithson et al.*, 1981], but is the same as a previous estimate for the conterminous United States [*Braile et al.*, 1989].

We have adopted the definition of the top of the upper mantle as that depth where the seismic velocity exceeds 7.6 km/s. This upper mantle velocity is frequently referred to as the Pn velocity, for "normal *P* (compressional) wave". Our compilation of the *Pn* velocities shows a range of values from 7.6 to 8.8 km/s (Figure 4). The unweighted average *Pn* velocity is 8.07 km/s, and the standard deviation is 0.21 km/s. This estimate compares well with previous compilations of *Pn* velocity (Table 2). There are two factors that appear to play a major role in determining upper mantle velocity: temperature and anisotropy. The effect of temperature can be clearly measured in active rift zones, such as the Kenya rift, where *Pn* velocities of 7.6-7.7 km/s have been reliably measured along the axis of the rift [*Mechie et al.*, 1994]. The existence of seismic anisotropy in the upper mantle has been well determined from oceanic and continental investigations that have consistently shown an azimuthal dependence of the *Pn* velocity [*Raitt et al.*, 1969; *Bamford*, 1977].

Seismic Velocities as a Function of Depth

In order to compare field measurements of crustal seismic velocities with laboratory measurements, we have made histograms of crustal velocities at 5-km depth intervals to a maximum depth of 50 km (Figure 5). The velocities taken at each depth were point values, not averages over a depth range, and exact values were determined in the case of velocity-depth gradient zones. There are insufficient data for the histograms to be meaningful at greater depths (Figure 2). The histograms at 5-km and 10-km depths are sharply peaked at 6.0-6.2 km/s, corresponding to seismic velocities that are typically reported for the crystalline upper crust. At 15-km and 20-km depths, the velocity distribution broadens considerably and seismic velocities greater than 6.3 km/s become more common. At a depth of 25 km, the velocity distribution is peaked once again, at a value of 6.6 km/s, indicating that typical middle crustal seismic velocities have been reached. In terms of common crustal nomenclature, by 25 km depth, we have passed through the "Conrad discontinuity," a gradational boundary that separates the upper crust (6.0-6.3 km/s) from the intermediate-velocity (6.6-6.8 km/s) middle crust (or in some cases lower crust) in many crustal sections.

The histograms between 30 km and 50 km show a continued trend to higher crustal velocities and at 40 km show a distinct bimodal pattern, with peaks at 6.8-6.9 km/s and 7.2 km/s. At

Table 2. Continental Seismic Properties

Reference	Region	Value
	Estimates of Continental Crustal Thicknesses	
Woollard [1959]	western Europe	35 km
Woollard [1959]	eastern Canada	40 km
Press [1966]	global range	28-65 km
Pavlenkova [1979]	Eurasia	42 km
Garland [1979]	global average	40 km
Braile et al. [1989]	North America (average)	36 km
Fowler [1990]	global average	35 km
Twiss and Moores [1992]	global average	35 km
This paper	unweighted global average	39 km
This paper	weighted global average	41 km
	*Estimates of Average Crustal Velocity**	
Mohorovicic [1909]	Yugoslavia	5.7 km/s
Press [1966]	global	6.4 km/s
Smithson et al. [1981]	global	6.3 km/s
Braile et al. [1989]	North America	6.44 km/s
Beloussov et al. [1991]	Eurasia	6.55 km/s
This paper	unweighted global average	6.45 km/s
This paper	weighted global average	6.45 km/s
	Estimates of Uppermost Mantle Velocity Pn	
Mohorovicic [1909]	Yugoslavia	7.75 km/s
Press [1966]	global	7.9-8.2 km/s
Garland [1979]	global	8.0 km/s
Braile et al. [1989]	North America (average)	8.0 km/s
Beloussov et al. [1991]	Eurasia	7.7-8.6 km/s
This paper	unweighted global average	8.07 km/s
This paper —	weighted global average	8.09 km/s

*No unconsolidated sediments.

45 km and 50 km depths, the modal velocity is 7.3 km/s, but a broad distribution of velocities persists (from 6.1-7.5 km/s), and the bimodal pattern can be weakly discerned. The increase in crustal velocity with depth in the crust can be seen in a perspective plot of these 10 histograms (Figure 6).

Tectonic Provinces

So far our discussion has been limited to a compilation of the entire worldwide data set. However, it has long been recognized that there are important correlations between crustal structure and tectonic province. We have therefore divided our data into five tectonic provinces (Figure 7) and have examined the properties of the crust in these provinces to search for trends. Shields and platforms occupy by far the largest area of continental crust (Figure 8). Orogens include the young, active mountain belts of the Alps, Andes, and Tibet and ancient orogens such as the Urals, Appalachians, and the Tien Shan, China. Continental arcs include the trans-Mexican volcanic belt, Cascades of North America, and active volcanic terrane of the western Pacific. Extended crust includes such regions as the Basin and Range of the western United States and much of western Europe. Rifts include East Africa, Lake Baikal, and the Rio Grande Rift. Extended crust and rifts are distinguished from each other in this study because they are traditionally considered separately in the geological literature and because these two types of crust have been the subject of intensive geophysical investigation which have distinguished differences in their seismic structure.

Shields and platforms show an average crustal thickness that is close to the worldwide average, 41.5 km. Extended crust, as the name implies, has been thinned and shows an average thickness of 30.5 km with a standard deviation of 5.3 km (Table 3). Orogens show a wide range of crustal thicknesses, ranging from about 30 km to 72 km. Rifts, both active and inactive, also show a broad range, from 18 km to 46 km. It should be emphasized that some of these ranges are obtained within a single tectonic province. For example, the crustal thickness within the Alps varies from about 35 km to as much as 60 km, and the Kenya rift shows crustal variations along strike of the rift that amount to 20-36 km. Thus significant variations occur along the strike of major geologic features.

As was mentioned above, the available global seismic refraction data have a nonuniform geographic distribution, which results in a strong geographical bias in such quantities as average crustal thickness. In order to correct the nonuniform data distribution, we have calculated crustal properties using a weighted average. Our approach is similar to that used by *Holbrook et al.* [1992] to calculate average crustal velocity. We estimate the following proportions of continental crust by area: 69% shield and platform; 15% old and young orogens; 9% extended crust; 6% magmatic arc; 1% rift. Mean values of crustal thickness, average crustal velocity, and Pn (upper mantle) velocity are listed in Table 3 for each of these crustal types, as are the weighted values determined from the five crustal types. This procedure corrects for the overrepresentation of crustal measurements in regions of extended crust, such as western Europe and the Basin and Range of the western United States, and the lack of measurements from Africa, South America, and Antarctica. The weighted mean crustal thickness of 41 km is 2 km thicker than the simple arithmetic mean of 39 km. We believe that the weighted values more accurately characterize average continental crust.

Vast portions of the continental crust are Precambrian shields and platforms (Figure 8), whereas much seismic exploration has concentrated in the younger crust of western Europe and the coastal regions of North America. Thus some previous studies have overemphasized the significance of the crustal structure of Phanerozoic crust. Precambrian crust is more "typical" of the continental crust than is Phanerozoic crust. We note that the crustal structure of Precambrian crust, which spans the period 0.6 Ga to 3.8 Ga, appears to show variations with age of the crust. *Drummond* [1988] and *Durrheim and Mooney* [1991, 1992] present evidence that most Proterozoic crust has a thickness of 40-55 km and a substantial high-velocity (7 km/s) layer at its base, while Archean crust is only 27-40 km thick (except at collisional boundaries) and generally lacks the basal high-velocity layer. *Durrheim and Mooney* [1994] argue that there are also differences in major and minor trace elements between Archean and Proterozoic crust. The secular change in

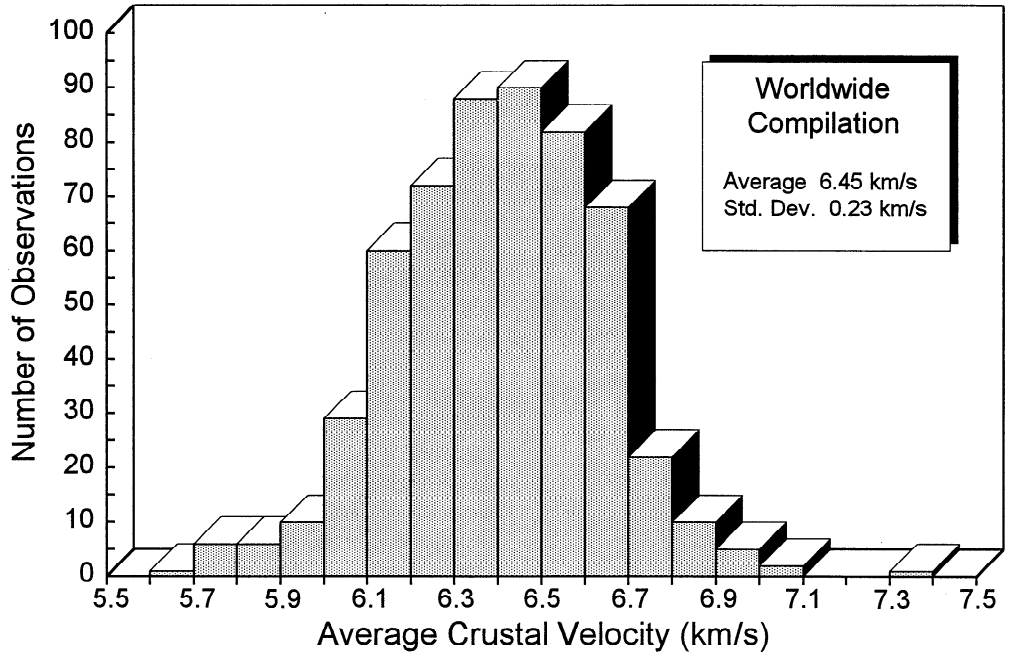

Figure 3. Histogram of average crustal velocity. Locations of data are shown in Figure 1. The weighted average crustal velocity is 6.45 km/s ± 0.21 km/s.

crustal properties is attributed by them to a decline in mantle temperature, which plays a major role in the magmatic and rheologic processes of crustal evolution.

The seismic structure of the crust described above provides important constraints on the composition and evolution of the crust. We rely on laboratory measurements of rock types commonly found in the continental crust to guide our interpretation of crustal composition. In order to compare velocity-pressure data with velocity-depth data, a weighted reference velocity depth function has been made from the average of the five tectonic provinces (Table 3 and Figure 9). Note that the velocity-depth functions of Figure 9 do not indicate velocity discontinuities in the crust, because discontinuities are smoothed by the averaging process. It is perhaps surprising that the calculated standard deviations are consistent with depth in view of the expected decreasing resolution of seismic velocity in the lower crust. This consistency may be attributed to greater lithologic diversity in the upper and middle crust (where velocity resolution is higher) as compared to the more homogeneous lower crust.

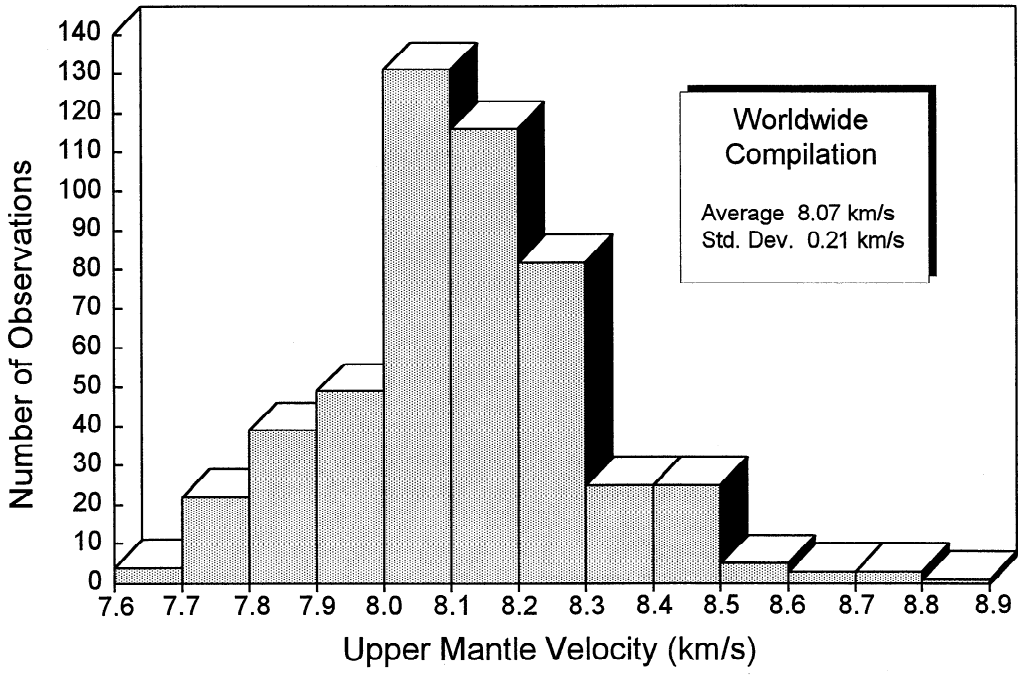

Figure 4. Histogram of uppermost mantle velocity (*Pn*). Locations of data are shown in Figure 1. The weighted average *Pn* velocity is 8.09 km/s ± 0.20 km/s.

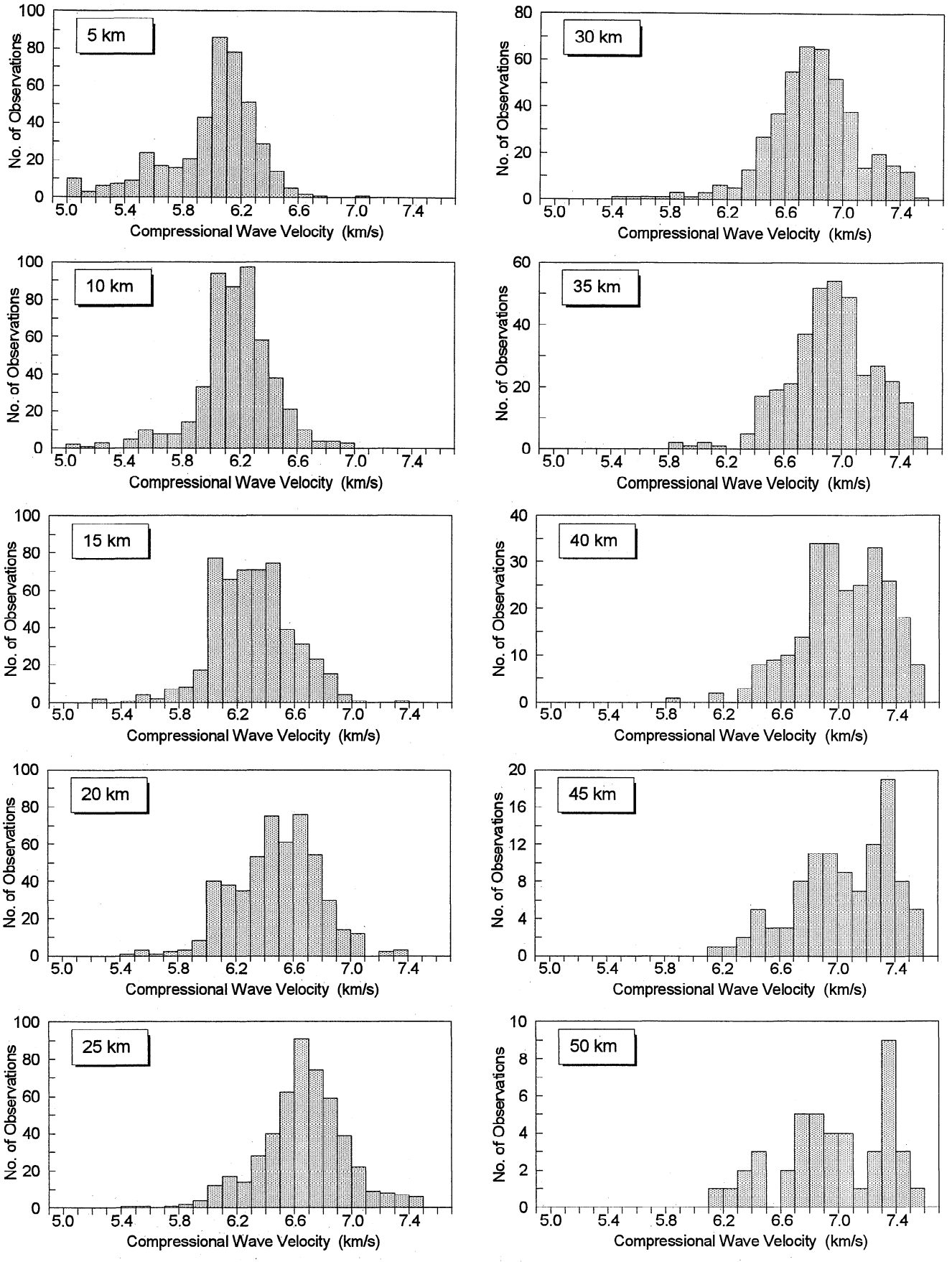

Figure 5. Histograms of crustal velocity at 5-km depth intervals. Locations of data are shown in Figure 1. Data have not been sorted by geologic or tectonic setting or crustal age. Shallow crustal velocities less than 5.0 km/s, corresponding to sedimentary rocks, and sub-Moho velocities greater than 7.5 km/s have been excluded.

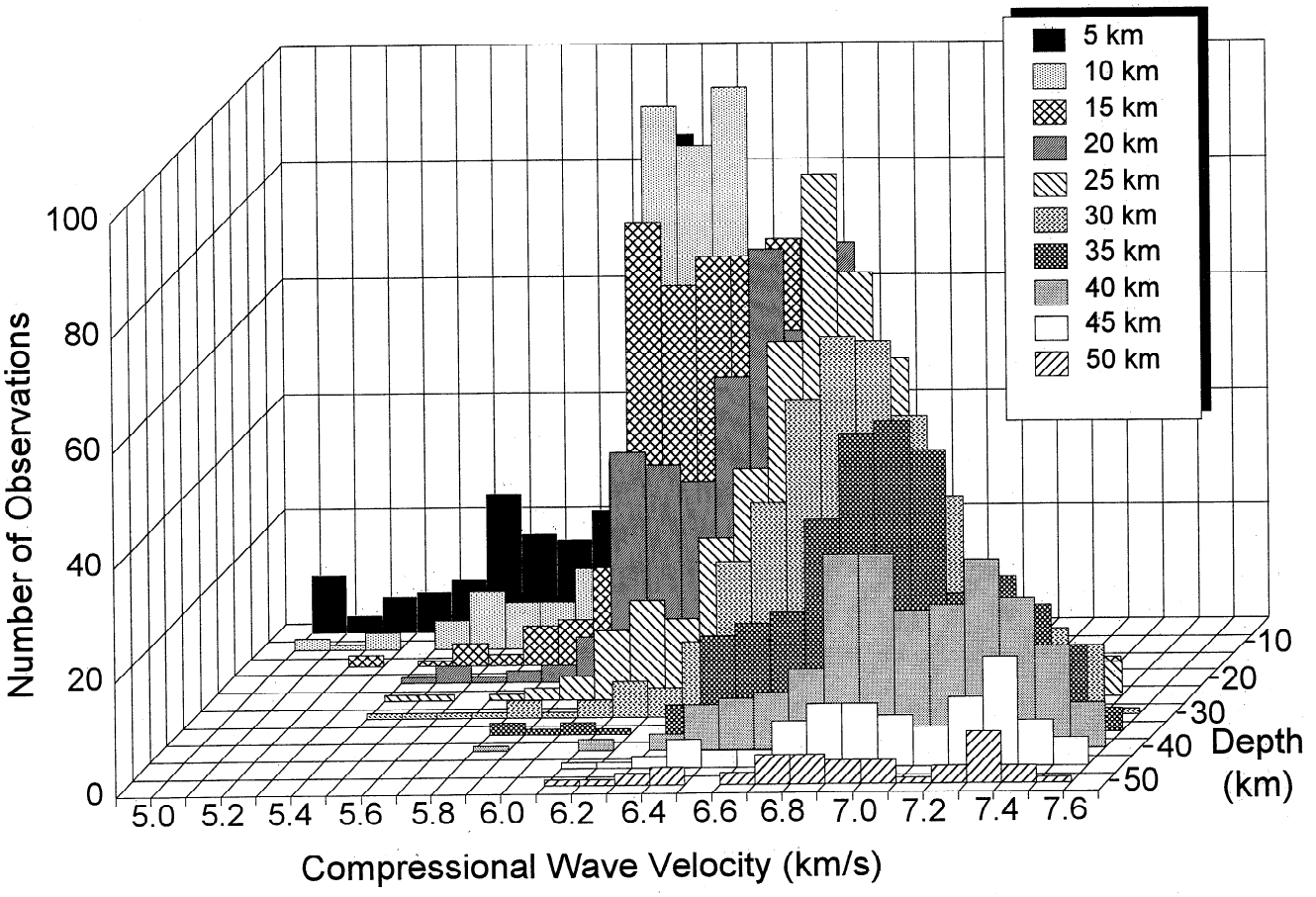

Figure 6. Perspective plot of the same data as shown in Figure 5, with the deep crust (50 km) in the foreground. A bimodal distribution in seismic velocity is visible at depths of 40-50 km, as are the increasing number of observations and the decrease in average crustal velocity at shallow depths.

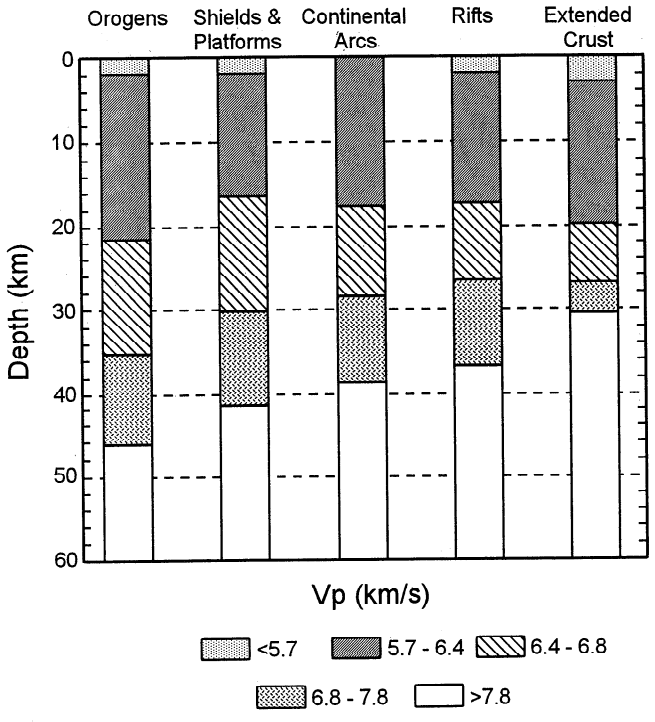

Figure 7. Average crustal structure for six tectonic provinces.

Velocities in Crystalline Rocks

The petrologic interpretation of seismic velocity distributions within the continental crust requires a detailed knowledge of seismic properties of a wide variety of rock types. Beginning with the benchmark papers of *Birch* [1960, 1961], a number of investigators have published measurements of wave velocities for rocks at sufficiently high pressure, and occasionally at both high pressure and temperature, to be useful in continental seismic investigations [e.g., *Christensen*, 1965; *Kern*, 1978; *Christensen*, 1979]. These studies have reported velocities for many rock types believed to be important constituents of the Earth's crust and upper mantle. An accumulation of a large number of new laboratory velocity measurements, presented for the first time in this paper, opens the way for a new interpretation of crustal seismic velocity structure in terms of petrology. A major objective of this study, which has been in progress for over a decade, has been to obtain detailed experimental data on the effects of mineralogy, chemistry, and metamorphic grade on seismic velocities. Over 3000 new runs measuring compressional wave velocities to pressures of 1 GPa (equivalent to crustal depths of 35 km) have been carried out. This has provided much needed information on average velocities and expected ranges of velocities for common crystalline rocks of the continental crust (Table 4).

Rock classification schemes allow for significant ranges in

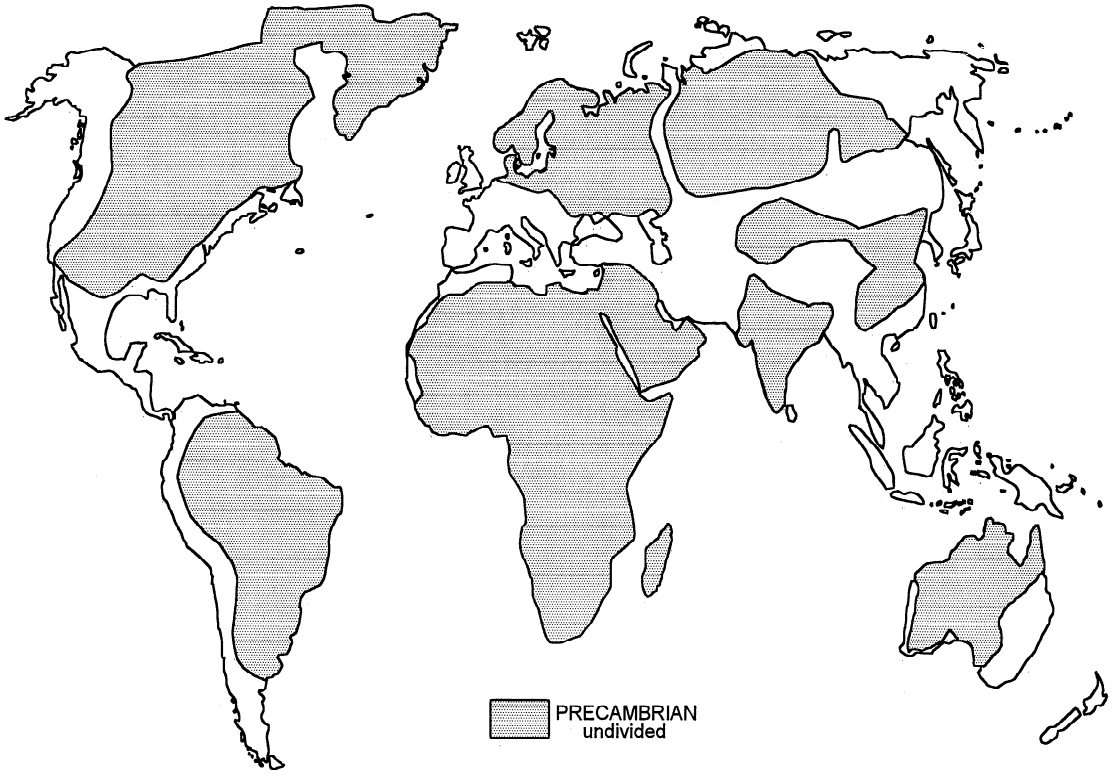

Figure 8. Map of Precambrian crust combined from individual country maps and summaries by *Windley* [1984] and *Goodwin* [1991]. The Precambrian of East Antarctica is not shown.

mineralogy for most common rock types. Thus even relatively simple lithologies, such as granite and gabbro, have variable elastic properties and reported velocities for a few samples are unlikely to adequately define the properties of these rocks. Owing to their complex mineralogy, this variability is even more critical for many metamorphic rocks. Velocity histograms for most rock types included in our compilation show normal distributions as is illustrated in Figure 10 for mafic granulite.

The samples selected for this study come from diverse tectonic settings and have a global distribution. Classification was based on petrographic examinations of thin sections and chemical analyses. Many previously published velocities were not included in our compilation because chemistry and detailed

Table 3. Velocities and Crustal Thickness for Tectonic Provinces and Average Continental Crust

Crustal Property	Orogens	Shields and Platforms	Continental Arcs	Rifts	Extended Crust	Average* Crust
Vp at 5 km	5.69 ± 0.67	5.68 ± 0.81	5.80 ± 0.34	5.64 ± 0.64	5.59 ± 0.88	5.95 ± 0.73†
Vp at 10 km	6.06 ± 0.39	6.10 ± 0.40	6.17 ± 0.34	6.05 ± 0.18	6.02 ± 0.45	6.21 ± 0.27†
Vp at 15 km	6.22 ± 0.32	6.32 ± 0.26	6.38 ± 0.33	6.29 ± 0.19	6.31 ± 0.32	6.31 ± 0.27
Vp at 20 km	6.38 ± 0.34	6.48 ± 0.26	6.55 ± 0.28	6.51 ± 0.23	6.53 ± 0.34	6.47 ± 0.28
Vp at 25 km	6.53 ± 0.39	6.65 ± 0.27	6.69 ± 0.28	6.72 ± 0.35	6.69 ± 0.30	6.64 ± 0.29
Vp at 30 km	6.68 ± 0.43	6.80 ± 0.27	6.84 ± 0.30	6.94 ± 0.37	6.89 ± 0.40	6.78 ± 0.30
Vp at 35 km	6.81 ± 0.40	6.96 ± 0.30	6.99 ± 0.29	7.12 ± 0.33	6.93 ± 0.46	6.93 ± 0.32
Vp at 40 km	6.92 ± 0.44	7.11 ± 0.33	7.14 ± 0.25	7.12 ± 0.30	—	7.02 ± 0.32
Vp at 45 km	6.96 ± 0.43	7.22 ± 0.39	—	—	—	7.09 ± 0.35
Vp at 50 km	6.99 ± 0.52	—	—	—	—	7.14 ± 0.38
Crustal thickness	46.3 ± 9.5	41.5 ± 5.8	38.7 ± 9.6	36.2 ± 7.9	30.5 ± 5.3	41.0 ± 6.2
Average crustal velocity	6.39 ± 0.25	6.42 ± 0.20	6.44 ± 0.25	6.36 ± 0.23	6.21 ± 0.22	6.45 ± 0.21†
Pn velocity	8.01 ± 0.22	8.13 ± 0.19	7.95 ± 0.23	7.93 ± 0.15	8.02 ± 0.19	8.09 ± 0.20

Velocities in km/s and thickness in km.

*Weighted average (69% shields and platforms, 15% orogens, 9% extended crust, 6% continental arcs, 1% rifts).

†Sedimentary sections have been removed from upper 10 km.

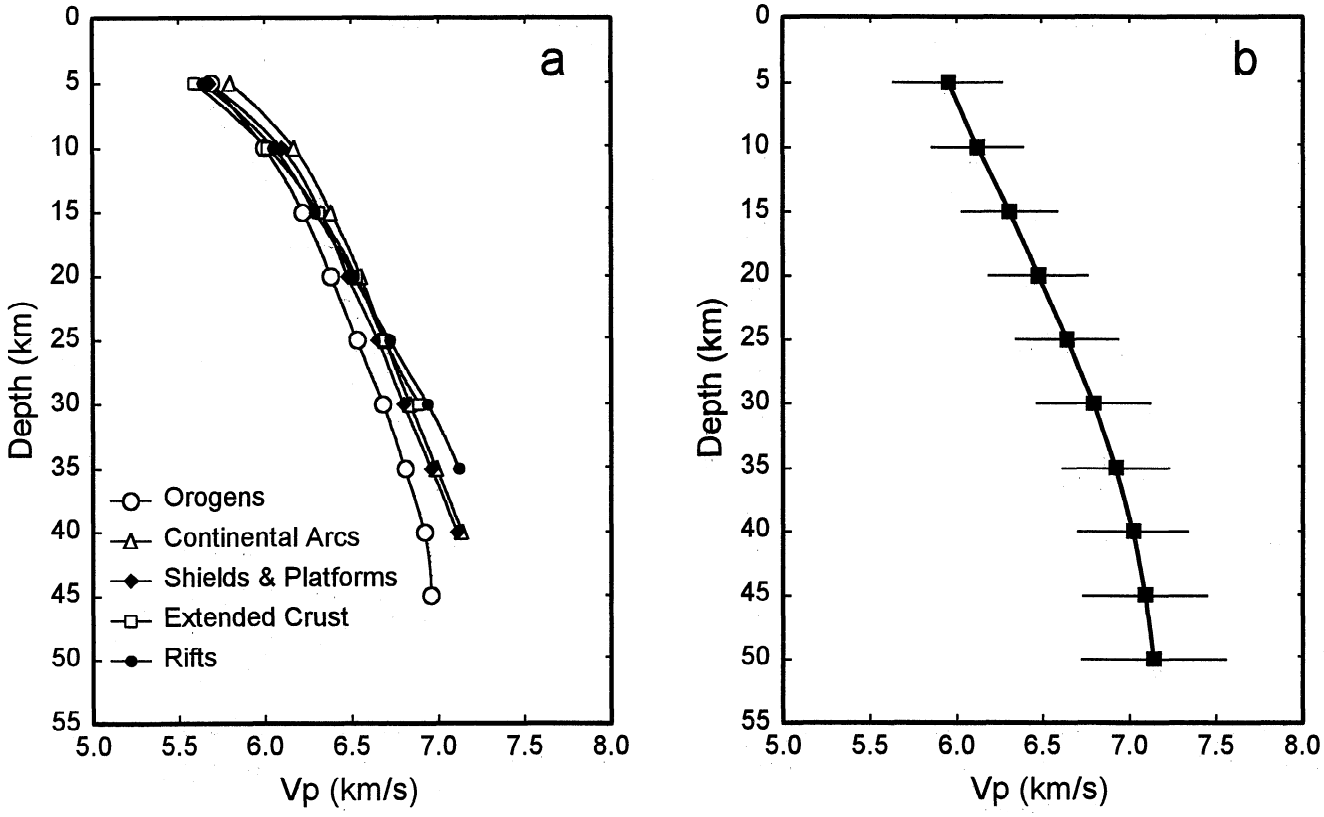

Figure 9. Average velocities versus depth for (a) five tectonic provinces and (b) reference average crustal model compiled from weighted tectonic province velocities at 5-km intervals. Horizontal bars in Figure 9b represent ± one standard deviation. The same data have been used as appear in the histograms of Figure 5. The average crustal model (Figure 9b) will be compared with laboratory-measured velocities of rock samples as a function of pressure.

petrography were not reported. Also because an important focus of this study is the deep continental crust, measurements included in Table 4 were all made to hydrostatic pressures of 1 GPa. The number of samples selected for a given category was dictated by their mineral variability and their availability. For relatively simple monomineralic rocks, only a few samples were studied; however, care was taken to select samples free of secondary alteration.

The number of categories into which the rocks were subdivided was kept to a minimum. Because of the limited lithologic resolution of seismic refraction studies, the use of more detailed rock classification schemes, such as those containing metamorphic subfacies, would serve little purpose. In Table 4, granites and granodiorites have been grouped together, as have gabbros, norites, and troctolites. The metagraywackes range in grade from zeolite to greenschist facies. The quartz mica schists include a variety of pelitic schists of the amphibolite facies, often containing garnet, staurolite, and/or kyanite. The tonalite gneisses, containing biotite, plagioclase, and quartz ± hornblende, are the common "gray gneisses" of many crustal sections. The paragranulites, of probable supracrustal origin as graywackes, contain plagioclase, quartz, garnet ± pyroxene ± kyanite ± sillimanite ± biotite. The metamorphosed mafic rocks have been classified into conventional facies assemblages, with mafic granulites subdivided into garnet-free and garnet-bearing rocks. The felsic granulites include acid feldspathic granulites and charnockitic rocks containing plagioclase mantled with microperthite, quartz, two pyroxenes ± hornblende ± garnet. The anorthosites have been separated by texture into igneous and metamorphic anorthosite. The marbles are primarily calcite bearing.

The pulse transmission technique for measuring velocities has been in use for many years [e.g., *Hughes and Maurette*, 1956; *Birch*, 1960, *Christensen*, 1965]. Experimental details of sample preparation, the electronics employed in the velocity measurements, and the pressure apparatus are given by *Christensen* [1985]. A variable mercury delay line was used for time measurements. This is important for precision, since, as with seismic records, there is a gradual onset of the first motion observed on the oscilloscope screen [*Birch*, 1960]. The signal through the calibrated delay line, which has a similar shape to the arrival from the sample, is superimposed on the transmitted signal from the rocks, eliminating much of the uncertainty of picking first arrivals. Thus, even through several laboratory technicians have taken the velocity measurements over several years, the repeatability of a given velocity measurement is of the order of a few tenths of a percent [*Christensen*, 1985], and observed variabilities within given rock types, or from one rock type to another, are not related to operator error in picking the first arrivals. The accuracy of each velocity measurement is better than 1%. Velocities at pressures greater than 1 GPa were obtained by extrapolation of the linear velocity-pressure curves measured between 600 MPa and 1 GPa. Velocities obtained in this manner agree well with limited velocity measurements in crystalline rocks to 3 GPa [*Christensen*, 1974].

At pressures found in the deep crust, the effect of compres-

Table 4. Densities and Compressional Wave Velocities as Functions of Temperature and Depth

Name		5 km					10 km					15 km					20 km					25 km				
Specimens (S)		ρ,	Room	Low	Avg	High	ρ,	Room	Low	Avg	High	ρ,	Room	Low	Avg	High	ρ,	Room	Low	Avg	High	ρ,	Room	Low	Avg	High
Rocks (R)		kg/m³	20°C	64°C	84°C	138°C	kg/m³	20°C	116°C	157°C	263°C	kg/m³	20°C	160°C	225°C	381°C	kg/m³	20°C	200°C	309°C	501°C	kg/m³	20°C	247°C	389°C	645°C
Andesite (AND)																										
S=30	Avg	2627	5.429	5.393	5.381	5.351	2630	5.627	5.561	5.538	5.477	2633	5.731	5.640	5.603	5.514	2635	5.800	5.686	5.623	5.514	2638	5.851	5.710	5.629	5.483
R=10	S.D.	71	0.280	0.280	0.280	0.280	70	0.239	0.239	0.239	0.239	70	0.227	0.227	0.227	0.227	70	0.224	0.224	0.224	0.224	69	0.224	0.224	0.224	0.224
Basalt (BAS)																										
S=415	Avg	2878	5.877	5.852	5.845	5.823	2883	5.954	5.908	5.892	5.851	2889	6.003	5.940	5.915	5.854	2894	6.039	5.961	5.918	5.843	2899	6.067	5.971	5.915	5.815
R=149	S.D.	144	0.547	0.547	0.547	0.547	144	0.543	0.543	0.543	0.543	144	0.542	0.542	0.542	0.542	144	0.541	0.541	0.541	0.541	144	0.540	0.540	0.540	0.540
Diabase (DIA)																										
S=54	Avg	2946	6.673	6.648	6.640	6.619	2952	6.719	6.674	6.658	6.617	2957	6.747	6.685	6.659	6.599	2962	6.765	6.687	6.645	6.570	2967	6.779	6.683	6.628	6.528
R=18	S.D.	85	0.253	0.253	0.253	0.253	85	0.245	0.245	0.245	0.245	85	0.239	0.239	0.239	0.239	85	0.235	0.235	0.235	0.235	85	0.232	0.232	0.232	0.232
Granite-Granodiorite (GRA)																										
S=134	Avg	2654	6.215	6.179	6.182	6.161	2661	6.287	6.221	6.226	6.184	2667	6.321	6.230	6.234	6.173	2673	6.344	6.230	6.224	6.149	2679	6.361	6.220	6.209	6.110
R=52	S.D.	24	0.135	0.135	0.135	0.135	24	0.125	0.125	0.125	0.125	24	0.124	0.124	0.124	0.124	24	0.124	0.124	0.124	0.124	24	0.125	0.125	0.125	0.125
Diorite (DIO)																										
S=24	Avg	2810	6.443	6.418	6.410	6.389	2815	6.528	6.483	6.467	6.426	2820	6.575	6.513	6.487	6.427	2825	6.608	6.530	6.487	6.412	2831	6.633	6.536	6.481	6.381
R=8	S.D.	85	0.167	0.167	0.167	0.167	85	0.155	0.155	0.155	0.155	85	0.144	0.144	0.144	0.144	85	0.134	0.134	0.134	0.134	85	0.126	0.126	0.126	0.126
Gabbro-Norite-Troctolite (GAB)																										
S=187	Avg	2966	7.096	7.060	7.048	7.018	2971	7.167	7.101	7.078	7.017	2975	7.210	7.118	7.081	6.992	2981	7.240	7.126	7.063	6.954	2985	7.262	7.122	7.041	6.895
R=69	S.D.	71	0.246	0.246	0.246	0.246	70	0.247	0.247	0.247	0.247	70	0.248	0.248	0.248	0.248	69	0.250	0.250	0.250	0.250	68	0.251	0.251	0.251	0.251
Metagraywacke (MGW)																										
S=87	Avg	2615	5.369	5.344	5.336	5.315	2621	5.522	5.477	5.461	5.420	2627	5.624	5.561	5.536	5.475	2632	5.701	5.623	5.580	5.505	2638	5.764	5.668	5.613	5.513
R=29	S.D.	112	0.615	0.615	0.615	0.615	112	0.564	0.564	0.564	0.564	112	0.519	0.519	0.519	0.519	112	0.479	0.479	0.479	0.479	112	0.443	0.443	0.443	0.443
Slate (SLT)																										
S=30	Avg	2801	6.098	6.073	6.065	6.044	2807	6.172	6.127	6.111	6.070	2813	6.227	6.164	6.139	6.078	2818	6.268	6.190	6.148	6.073	2824	6.302	6.206	6.151	6.051
R=10	S.D.	28	0.131	0.131	0.131	0.131	28	0.124	0.124	0.124	0.124	28	0.117	0.117	0.117	0.117	28	0.110	0.110	0.110	0.110	28	0.103	0.103	0.103	0.103
Phyllite (PHY)																										
S=144	Avg	2728	6.105	6.080	6.073	6.052	2734	6.210	6.164	6.148	6.107	2740	6.260	6.197	6.172	6.111	2745	6.292	6.214	6.171	6.096	2751	6.316	6.220	6.165	6.065
R=48	S.D.	58	0.258	0.258	0.258	0.258	58	0.206	0.206	0.206	0.206	58	0.183	0.183	0.183	0.183	58	0.168	0.168	0.168	0.168	58	0.158	0.158	0.158	0.158
Zeolite Facies Basalt (BZE)																										
S=57	Avg	2916	6.277	6.253	6.245	6.224	2922	6.368	6.323	6.307	6.266	2927	6.425	6.363	6.337	6.277	2932	6.465	6.387	6.344	6.269	2937	6.495	6.399	6.344	6.244
R=19	S.D.	81	0.269	0.269	0.269	0.269	81	0.261	0.261	0.261	0.261	81	0.257	0.257	0.257	0.257	81	0.254	0.254	0.254	0.254	81	0.252	0.252	0.252	0.252

Table 4 (continued)

Name		30 km					35 km					40 km					45 km					50 km				
Specimens (S)		ρ,	Room	Low	Avg	High	ρ,	Room	Low	Avg	High	ρ,	Room	Low	Avg	High	ρ,	Room	Low	Avg	High	ρ,	Room	Low	Avg	High
Rocks (R)		kg/m³	20°C	291°C	467°C	786°C	kg/m³	20°C	333°C	542°C	925°C	kg/m³	20°C	371°C	615°C	065°C	kg/m³	20°C	408°C	689°C	204°C	kg/m³	20°C	445°C	762°C	344°C
Andesite (AND)																										
S=30	Avg	2641	5.893	5.727	5.627	5.445	2643	5.928	5.738	5.619	5.401	2646	5.964	5.752	5.613	5.357	2649	5.999	5.766	5.606	5.313	2652	6.034	5.781	5.600	5.268
R=10	S.D.	69	0.226	0.226	0.226	0.226	70	0.229	0.229	0.229	0.229	70	0.232	0.232	0.232	0.232	71	0.236	0.236	0.236	0.236	71	0.241	0.241	0.241	0.241
Basalt (BAS)																										
S=415	Avg	2904	6.090	5.977	5.908	5.784	2910	6.110	5.981	5.899	5.750	2915	6.130	5.986	5.890	5.715	2920	6.150	5.991	5.882	5.681	2926	6.170	5.997	5.873	5.646
R=149	S.D.	144	0.540	0.540	0.540	0.540	144	0.539	0.539	0.539	0.539	144	0.539	0.539	0.539	0.539	144	0.539	0.539	0.539	0.539	144	0.539	0.539	0.539	0.539
Diabase (DIA)																										
S=54	Avg	2973	6.790	6.677	6.608	6.484	2978	6.799	6.669	6.587	6.438	2983	6.807	6.663	6.567	6.392	2988	6.816	6.656	6.547	6.346	2993	6.824	6.650	6.527	6.300
R=18	S.D.	85	0.230	0.230	0.230	0.230	85	0.228	0.228	0.228	0.228	85	0.227	0.227	0.227	0.227	85	0.225	0.225	0.225	0.225	85	0.224	0.224	0.224	0.224
Granite-Granodiorite (GRA)																										
S=134	Avg	2686	6.374	6.208	6.192	6.067	2692	6.384	6.194	6.173	6.024	2698	6.395	6.183	6.155	5.979	2704	6.405	6.172	6.136	5.935	2710	6.415	6.161	6.118	5.891
R=52	S.D.	24	0.126	0.126	0.126	0.126	24	0.128	0.128	0.128	0.128	24	0.130	0.130	0.130	0.130	24	0.132	0.132	0.132	0.132	24	0.134	0.134	0.134	0.134
Diorite (DIO)																										
S=24	Avg	2836	6.652	6.538	6.470	6.345	2841	6.668	6.538	6.457	6.307	2847	6.684	6.540	6.444	6.269	2852	6.701	6.541	6.432	6.231	2857	6.717	6.543	6.420	6.193
R=8	S.D.	85	0.120	0.120	0.120	0.120	85	0.114	0.114	0.114	0.114	85	0.109	0.109	0.109	0.109	85	0.105	0.105	0.105	0.105	85	0.100	0.100	0.100	0.100
Gabbro-Norite-Troctolite (GAB)																										
S=187	Avg	2991	7.282	7.116	7.015	6.834	2995	7.296	7.106	6.987	6.769	3000	7.311	7.100	6.960	6.704	3005	7.326	7.093	6.933	6.639	3010	7.340	7.087	6.906	6.574
R=69	S.D.	67	0.252	0.252	0.252	0.252	67	0.254	0.254	0.254	0.254	66	0.255	0.255	0.255	0.255	66	0.257	0.257	0.257	0.257	66	0.259	0.259	0.259	0.259
Metagraywacke (MGW)																										
S=87	Avg	2644	5.818	5.704	5.635	5.511	2650	5.865	5.735	5.653	5.504	2656	5.912	5.767	5.672	5.497	2662	5.959	5.800	5.691	5.490	2668	6.007	5.833	5.709	5.482
R=29	S.D.	112	0.411	0.411	0.411	0.411	112	0.383	0.383	0.383	0.383	112	0.357	0.357	0.357	0.357	112	0.333	0.333	0.333	0.333	112	0.311	0.311	0.311	0.311
Slate (SLT)																										
S=30	Avg	2630	6.329	6.216	6.147	6.023	2636	6.353	6.223	6.142	5.992	2842	6.377	6.232	6.137	5.961	2848	6.401	6.241	6.132	5.931	2854	6.424	6.251	6.127	5.900
R=10	S.D.	28	0.097	0.097	0.097	0.097	28	0.092	0.092	0.092	0.092	28	0.087	0.087	0.087	0.087	28	0.083	0.083	0.083	0.083	28	0.081	0.081	0.081	0.081
Phyllite (PHY)																										
S=144	Avg	2757	6.335	6.221	6.152	6.028	2763	6.350	6.220	6.139	5.989	2769	6.366	6.221	6.126	5.950	2775	6.381	6.222	6.113	5.912	2781	6.397	6.223	6.100	5.873
R=48	S.D.	58	0.150	0.150	0.150	0.150	58	0.144	0.144	0.144	0.144	58	0.138	0.138	0.138	0.138	58	0.133	0.133	0.133	0.133	58	0.128	0.128	0.128	0.128
Zeolite Facies Basalt (BZE)																										
S=57	Avg	2943	6.519	6.406	6.337	6.213	2948	6.539	6.409	6.328	6.178	2953	6.559	6.414	6.319	6.144	2958	6.579	6.420	6.310	6.109	2963	6.598	6.425	6.301	6.074
R=19	S.D.	81	0.251	0.251	0.251	0.251	81	0.250	0.250	0.250	0.250	81	0.250	0.250	0.250	0.250	81	0.250	0.250	0.250	0.250	81	0.250	0.250	0.250	0.250

Table 4. (continued)

Name		5 km					10 km					15 km					20 km					25 km				
Specimens (S)		ρ,	Room	Low	Avg	High	ρ,	Room	Low	Avg	High	ρ,	Room	Low	Avg	High	ρ,	Room	Low	Avg	High	ρ,	Room	Low	Avg	High
Rocks (R)		kg/m³	20°C	64°C	84°C	138°C	kg/m³	20°C	116°C	157°C	263°C	kg/m³	20°C	160°C	225°C	381°C	kg/m³	20°C	200°C	309°C	501°C	kg/m³	20°C	247°C	389°C	645°C
Prehnite-Pumpellyite Facies Basalt (BPP)																										
S=45	Avg	2829	6.281	6.256	6.248	6.227	2835	6.377	6.332	6.316	6.275	2840	6.436	6.374	6.349	6.288	2845	6.477	6.399	6.357	6.282	2850	6.510	6.414	6.358	6.258
R=15	S.D.	102	0.399	0.399	0.399	0.399	102	0.361	0.361	0.361	0.361	102	0.342	0.342	0.342	0.342	102	0.329	0.329	0.329	0.329	102	0.320	0.320	0.320	0.320
Greenschist Facies Basalt (BGR)																										
S=63	Avg	2991	6.680	6.655	6.647	6.626	2996	6.804	6.759	6.743	6.702	3001	6.863	6.801	6.776	6.715	3006	6.899	6.821	6.778	6.703	3012	6.925	6.828	6.773	6.673
R=21	S.D.	98	0.273	0.273	0.273	0.273	98	0.249	0.249	0.249	0.249	98	0.244	0.244	0.244	0.244	98	0.242	0.242	0.242	0.242	98	0.241	0.241	0.241	0.241
Granite Gneiss (GGN)																										
S=189	Avg	2662	6.027	6.002	5.994	5.973	2669	6.155	6.110	6.094	6.052	2675	6.213	6.150	6.125	6.064	2681	6.251	6.173	6.130	6.055	2687	6.279	6.183	6.128	6.028
R=63	S.D.	46	0.204	0.204	0.204	0.204	46	0.146	0.146	0.146	0.146	46	0.123	0.123	0.123	0.123	46	0.110	0.110	0.110	0.110	46	0.100	0.100	0.100	0.100
Biotite (Tonalite) Gneiss (BGN)																										
S=318	Avg	2746	6.137	6.113	6.105	6.084	2753	6.242	6.197	6.181	6.139	2759	6.291	6.229	6.204	6.143	2766	6.324	6.246	6.204	6.129	2772	6.348	6.252	6.196	6.096
R=106	S.D.	71	0.208	0.208	0.208	0.208	71	0.183	0.183	0.183	0.183	71	0.175	0.175	0.175	0.175	71	0.172	0.172	0.172	0.172	71	0.169	0.169	0.169	0.169
Mica Quartz Schist (QSC)																										
S=111	Avg	2830	6.194	6.169	6.161	6.140	2836	6.342	6.297	6.281	6.240	2843	6.414	6.351	6.326	6.265	2849	6.461	6.383	6.340	6.265	2856	6.495	6.399	6.344	6.244
R=37	S.D.	129	0.348	0.348	0.348	0.348	129	0.354	0.354	0.354	0.354	129	0.363	0.363	0.363	0.363	129	0.370	0.370	0.370	0.370	129	0.375	0.375	0.375	0.375
Amphibolite (AMP)																										
S=171	Avg	2992	6.790	6.757	6.746	6.718	2996	6.909	6.849	6.828	6.773	3001	6.962	6.879	6.845	6.764	3006	6.997	6.893	6.836	6.737	3011	7.021	6.893	6.819	6.686
R=57	S.D.	83	0.261	0.261	0.261	0.261	83	0.242	0.242	0.242	0.242	83	0.238	0.238	0.238	0.238	83	0.238	0.238	0.238	0.238	83	0.238	0.238	0.238	0.238
Felsic Granulite (FGR)																										
S=96	Avg	2755	6.355	6.321	6.311	6.283	2761	6.433	6.373	6.352	6.297	2766	6.477	6.393	6.360	6.279	2771	6.506	6.402	6.345	6.246	2776	6.529	6.401	6.327	6.194
R=32	S.D.	76	0.133	0.133	0.133	0.133	76	0.128	0.128	0.128	0.128	76	0.129	0.129	0.129	0.129	76	0.130	0.130	0.130	0.130	76	0.131	0.131	0.131	0.131
Paragranulite (PGR)																										
S=42	Avg	2761	6.279	6.246	6.235	6.207	2766	6.373	6.312	6.291	6.236	2771	6.418	6.335	6.301	6.220	2776	6.447	6.343	6.286	6.186	2782	6.470	6.341	6.268	6.134
R=14	S.D.	56	0.191	0.191	0.191	0.191	56	0.155	0.155	0.155	0.155	56	0.143	0.143	0.143	0.143	56	0.138	0.138	0.138	0.138	56	0.136	0.136	0.136	0.136
Anorthositic Granulite (AGR)																										
S=48	Avg	2751	6.831	6.798	6.787	6.759	2757	6.914	6.854	6.833	6.777	2762	6.955	6.872	6.838	6.757	2767	6.981	6.877	6.820	6.720	2772	7.003	6.874	6.800	6.667
R=16	S.D.	57	0.126	0.126	0.126	0.126	57	0.135	0.135	0.135	0.135	57	0.141	0.141	0.141	0.141	57	0.144	0.144	0.144	0.144	57	0.149	0.149	0.149	0.149
Mafic Granulite (MGR)																										
S=108	Avg	2977	6.789	6.756	6.746	6.718	2983	6.872	6.812	6.790	6.735	2988	6.915	6.832	6.798	6.717	2993	6.944	6.840	6.783	6.683	2998	6.965	6.836	6.762	6.629
R=36	S.D.	85	0.184	0.184	0.184	0.184	84	0.176	0.176	0.176	0.176	84	0.178	0.178	0.178	0.178	85	0.180	0.180	0.180	0.180	85	0.183	0.183	0.183	0.183

Table 4 (continued)

Name		30 km					35 km					40 km					45 km					50 km				
Specimens (S)		ρ,	Room	Low	Avg	High	ρ,	Room	Low	Avg	High	ρ,	Room	Low	Avg	High	ρ,	Room	Low	Avg	High	ρ,	Room	Low	Avg	High
Rocks (R)		kg/m³	20°C	291°C	467°C	786°C	kg/m³	20°C	333°C	542°C	925°C	kg/m³	20°C	371°C	615°C	065°C	kg/m³	20°C	408°C	689°C	204°C	kg/m³	20°C	445°C	762°C	344°C
Prehnite-Pumpellyite Facies Basalt (BPP)																										
S=45	Avg	2856	6.536	6.422	6.354	6.229	2861	6.557	6.427	6.346	6.197	2866	6.579	6.434	6.339	6.164	2871	6.600	6.441	6.332	6.131	2876	6.622	6.448	6.325	6.098
R=15	S.D.	102	0.313	0.313	0.313	0.313	102	0.307	0.307	0.307	0.307	102	0.302	0.302	0.302	0.302	102	0.296	0.296	0.296	0.296	102	0.292	0.292	0.292	0.292
Greenschist Facies Basalt (BGR)																										
S=63	Avg	3017	6.944	6.831	6.762	6.638	3022	6.960	6.830	6.749	6.599	3028	6.976	6.831	6.736	6.560	3033	6.991	6.832	6.723	6.522	3038	7.007	6.834	6.710	6.483
R=21	S.D.	98	0.240	0.240	0.240	0.240	98	0.240	0.240	0.240	0.240	98	0.239	0.239	0.239	0.239	98	0.239	0.239	0.239	0.239	98	0.240	0.240	0.240	0.240
Granite Gneiss (GGN)																										
S=189	Avg	2694	6.302	6.188	6.120	5.995	2700	6.320	6.190	6.109	5.959	2706	6.338	6.194	6.098	5.923	2712	6.356	6.197	6.088	5.887	2718	6.375	6.201	6.078	5.851
R=63	S.D.	46	0.094	0.094	0.094	0.094	46	0.088	0.088	0.088	0.088	46	0.084	0.084	0.084	0.084	46	0.081	0.081	0.081	0.081	46	0.078	0.078	0.078	0.078
Biotite (Tonalite) Gneiss (BGN)																										
S=318	Avg	2779	6.367	6.253	6.185	6.060	2785	6.382	6.252	6.170	6.021	2791	6.397	6.252	6.157	5.981	2798	6.412	6.252	6.143	5.942	2804	6.427	6.253	6.129	5.902
R=106	S.D.	71	0.168	0.168	0.168	0.168	71	0.167	0.167	0.167	0.167	71	0.167	0.167	0.167	0.167	71	0.166	0.166	0.166	0.166	71	0.166	0.166	0.166	0.166
Mica Quartz Schist (QSC)																										
S=111	Avg	2862	6.524	6.411	6.342	6.217	2869	6.547	6.417	6.335	6.186	2876	6.569	6.424	6.329	6.154	2883	6.592	6.433	6.323	6.122	2890	6.614	6.441	6.317	6.090
R=37	S.D.	129	0.378	0.378	0.378	0.378	129	0.381	0.381	0.381	0.381	129	0.385	0.385	0.385	0.385	129	0.388	0.388	0.388	0.388	129	0.392	0.392	0.392	0.392
Amphibolite (AMP)																										
S=171	Avg	3016	7.040	6.889	6.797	6.631	3021	7.055	6.882	6.773	6.574	3026	7.070	6.877	6.751	6.517	3031	7.085	6.873	6.727	6.459	3036	7.101	6.869	6.704	6.402
R=57	S.D.	83	0.238	0.238	0.238	0.238	83	0.239	0.239	0.239	0.239	83	0.240	0.240	0.240	0.240	83	0.241	0.241	0.241	0.241	83	0.242	0.242	0.242	0.242
Felsic Granulite (FGR)																										
S=96	Avg	2782	6.546	6.394	6.303	6.137	2787	6.560	6.387	6.278	6.079	2792	6.575	6.382	6.255	6.021	2797	6.589	6.377	6.231	5.963	2802	6.603	6.372	6.207	5.905
R=32	S.D.	76	0.133	0.133	0.133	0.133	76	0.134	0.134	0.134	0.134	76	0.136	0.136	0.136	0.136	76	0.138	0.138	0.138	0.138	76	0.140	0.140	0.140	0.140
Paragranulite (PGR)																										
S=42	Avg	2787	6.486	6.335	6.243	6.077	2792	6.499	6.326	6.218	6.018	2798	6.513	6.320	6.193	5.959	2803	6.526	6.314	6.168	5.900	2808	6.540	6.309	6.144	5.841
R=14	S.D.	56	0.135	0.135	0.135	0.135	56	0.135	0.135	0.135	0.135	56	0.134	0.134	0.134	0.134	56	0.134	0.134	0.134	0.134	56	0.134	0.134	0.134	0.134
Anorthositic Granulite (AGR)																										
S=48	Avg	2778	7.019	6.867	6.776	6.610	2783	7.031	6.858	6.749	6.550	2788	7.044	6.851	6.724	6.490	2794	7.057	6.844	6.698	6.431	2799	7.069	6.838	6.673	6.370
R=16	S.D.	57	0.153	0.153	0.153	0.153	57	0.156	0.156	0.156	0.156	57	0.160	0.160	0.160	0.160	57	0.164	0.164	0.164	0.164	57	0.168	0.168	0.168	0.168
Mafic Granulite (MGR)																										
S=108	Avg	3004	6.980	6.828	6.737	6.571	3009	6.992	6.819	6.710	6.511	3014	7.005	6.812	6.685	6.451	3019	7.018	6.805	6.659	6.392	3024	7.030	6.799	6.634	6.331
R=36	S.D.	84	0.186	0.186	0.186	0.186	85	0.188	0.188	0.188	0.188	85	0.191	0.191	0.191	0.191	85	0.193	0.193	0.193	0.193	85	0.196	0.196	0.196	0.196

Table 4. (continued)

Name		5 km					10 km					15 km					20 km					25 km				
Specimens (S)		ρ,	Room	Low	Avg	High	ρ,	Room	Low	Avg	High	ρ,	Room	Low	Avg	High	ρ,	Room	Low	Avg	High	ρ,	Room	Low	Avg	High
Rocks (R)		kg/m³	20°C	64°C	84°C	138°C	kg/m³	20°C	116°C	157°C	263°C	kg/m³	20°C	160°C	225°C	381°C	kg/m³	20°C	200°C	309°C	501°C	kg/m³	20°C	247°C	389°C	645°C
Mafic Garnet Granulite (GGR)																										
S=90	Avg	3121	7.021	6.987	6.977	6.949	3127	7.151	7.090	7.069	7.014	3132	7.208	7.125	7.091	7.010	3137	7.249	7.145	7.088	6.988	3142	7.277	7.149	7.075	6.942
R=30	S.D.	113	0.222	0.222	0.222	0.222	113	0.189	0.189	0.189	0.189	113	0.190	0.190	0.190	0.190	113	0.183	0.183	0.183	0.183	113	0.182	0.182	0.182	0.182
Mafic Eclogite (ECL)																										
S=54	Avg	3480	7.923	7.889	7.879	7.850	3484	8.019	7.958	7.936	7.880	3488	8.071	7.987	7.952	7.869	3491	8.107	8.001	7.944	7.842	3495	8.133	8.002	7.927	7.792
R=18	S.D.	70	0.187	0.187	0.187	0.187	70	0.176	0.176	0.176	0.176	70	0.171	0.171	0.171	0.171	70	0.168	0.168	0.168	0.168	70	0.166	0.166	0.166	0.166
Serpentinite (SER)																										
S=36	Avg	2571	5.310	5.266	5.253	5.216	2572	5.392	5.313	5.285	5.213	2576	5.457	5.348	5.304	5.198	2579	5.510	5.374	5.300	5.169	2583	5.555	5.387	5.291	5.117
R=12	S.D.	46	0.321	0.321	0.321	0.321	46	0.303	0.303	0.303	0.303	46	0.289	0.289	0.289	0.289	46	0.278	0.278	0.278	0.278	46	0.267	0.267	0.267	0.267
Quartzite (QTZ)																										
S=36	Avg	2646	5.936	5.900	5.889	5.859	2655	6.008	5.943	5.920	5.860	2662	6.046	5.956	5.920	5.833	2669	6.071	5.959	5.898	5.791	2677	6.090	5.951	5.872	5.729
R=12	S.D.	15	0.082	0.082	0.082	0.082	15	0.079	0.079	0.079	0.079	15	0.083	0.083	0.083	0.083	15	0.084	0.084	0.084	0.084	15	0.086	0.086	0.086	0.086
Calcite Marble (MBL)																										
S=30	Avg	2721	6.841	6.814	6.806	6.784	2725	6.889	6.841	6.825	6.781	2730	6.910	6.844	6.817	6.753	2734	6.923	6.841	6.797	6.718	2739	6.932	6.830	6.772	6.667
R=10	S.D.	14	0.131	0.131	0.131	0.131	14	0.124	0.124	0.124	0.124	14	0.123	0.123	0.123	0.123	14	0.123	0.123	0.123	0.123	14	0.123	0.123	0.123	0.123
Anorthosite (ANO)																										
S=63	Avg	2736	6.894	6.868	6.860	6.838	2739	6.966	6.918	6.901	6.858	2743	7.001	6.936	6.909	6.845	2748	7.025	6.943	6.899	6.820	2752	7.043	6.941	6.883	6.778
R=21	S.D.	40	0.212	0.212	0.212	0.212	40	0.206	0.206	0.206	0.206	40	0.203	0.203	0.203	0.203	40	0.203	0.203	0.203	0.203	40	0.203	0.203	0.203	0.203
Hornblendite (HBL)																										
S=6	Avg	3250	7.108	7.072	7.060	7.030	3252	7.188	7.123	7.100	7.041	3256	7.230	7.140	7.104	7.017	3260	7.258	7.146	7.085	6.977	3264	7.279	7.140	7.061	6.917
R=2	S.D.	1	0.035	0.035	0.035	0.035	1	0.005	0.005	0.005	0.005	1	0.010	0.010	0.010	0.010	1	0.021	0.021	0.021	0.021	1	0.029	0.029	0.029	0.029
Pyroxenite (PYX)																										
S=33	Avg	3270	7.712	7.676	7.665	7.635	3272	7.782	7.717	7.694	7.635	3276	7.828	7.738	7.702	7.615	3280	7.862	7.750	7.689	7.581	3284	7.888	7.750	7.670	7.527
R=11	S.D.	28	0.114	0.114	0.114	0.114	28	0.098	0.098	0.098	0.098	28	0.092	0.092	0.092	0.092	28	0.090	0.090	0.090	0.090	28	0.089	0.089	0.089	0.089
Dunite (DUN)																										
S=51	Avg	3309	8.237	8.201	8.190	8.160	3310	8.301	8.236	8.213	8.153	3313	8.336	8.247	8.210	8.123	3317	8.359	8.247	8.186	8.078	3321	8.374	8.236	8.156	8.013
R=17	S.D.	14	0.114	0.114	0.114	0.114	14	0.108	0.108	0.108	0.108	14	0.112	0.112	0.112	0.112	14	0.119	0.119	0.119	0.119	14	0.129	0.129	0.129	0.129

Table 4. (continued)

Name		30 km					35 km					40 km					45 km					50 km				
Specimens (S)		ρ,	Room	Low	Avg	High	ρ,	Room	Low	Avg	High	ρ,	Room	Low	Avg	High	ρ,	Room	Low	Avg	High	ρ,	Room	Low	Avg	High
Rocks (R)		kg/m³	20°C	291°C	467°C	786°C	kg/m³	20°C	333°C	542°C	925°C	kg/m³	20°C	371°C	615°C	065°C	kg/m³	20°C	408°C	689°C	204°C	kg/m³	20°C	445°C	762°C	344°
Mafic Garnet Granulite (GGR)																										
S=90	Avg	3148	7.297	7.146	7.054	6.888	3153	7.314	7.141	7.032	6.833	3158	7.331	7.138	7.011	6.777	3163	7.348	7.135	6.989	6.721	3168	7.364	7.133	6.968	6.665
R=30	S.D.	113	0.183	0.183	0.183	0.183	113	0.184	0.184	0.184	0.184	113	0.185	0.185	0.185	0.185	113	0.187	0.187	0.187	0.187	113	0.189	0.189	0.189	0.189
Mafic Eclogite (ECL)																										
S=54	Avg	3499	8.154	8.000	7.906	7.737	3503	8.170	7.994	7.883	7.680	3507	8.187	7.990	7.861	7.622	3511	8.203	7.987	7.838	7.565	3515	8.220	7.984	7.816	7.507
R=18	S.D.	70	0.165	0.165	0.165	0.165	70	0.165	0.165	0.165	0.165	70	0.164	0.164	0.164	0.164	70	0.164	0.164	0.164	0.164	70	0.164	0.164	0.164	0.164
Serpentinite (SER)																										
S=36	Avg	2586	5.593	5.395	5.275	5.058	2590	5.627	5.401	5.259	4.998	2594	5.661	5.409	5.243	4.937	2597	5.696	5.418	5.227	4.877	2601	5.730	5.427	5.212	4.816
R=12	S.D.	46	0.258	0.258	0.258	0.258	46	0.249	0.249	0.249	0.249	46	0.241	0.241	0.241	0.241	46	0.233	0.233	0.233	0.233	46	0.226	0.226	0.226	0.226
Quartzite (QTZ)																										
S=36	Avg	2684	6.104	5.941	5.842	5.664	2691	6.115	5.929	5.812	5.597	2698	6.127	5.919	5.783	5.531	2706	6.138	5.910	5.753	5.464	2713	6.150	5.901	5.723	5.397
R=12	S.D.	15	0.089	0.089	0.089	0.089	15	0.092	0.092	0.092	0.092	15	0.095	0.095	0.095	0.095	15	0.098	0.098	0.098	0.098	15	0.101	0.101	0.101	0.101
Calcite Marble (MBL)																										
S=30	Avg	2743	6.938	6.818	6.746	6.615	2748	6.942	6.805	6.719	6.562	2753	6.946	6.794	6.694	6.509	2758	6.950	6.783	6.667	6.456	2763	6.954	6.771	6.641	6.403
R=10	S.D.	14	0.123	0.123	0.123	0.123	14	0.123	0.123	0.123	0.123	14	0.124	0.124	0.124	0.124	14	0.124	0.124	0.124	0.124	14	0.125	0.125	0.125	0.125
Anorthosite (ANO)																										
S=63	Avg	2757	7.057	6.938	6.865	6.735	2761	7.067	6.931	6.845	6.688	2766	7.078	6.926	6.826	6.641	2770	7.089	6.921	6.806	6.595	2774	7.099	6.917	6.787	6.548
R=21	S.D.	40	0.203	0.203	0.203	0.203	40	0.204	0.204	0.204	0.204	40	0.205	0.205	0.205	0.205	40	0.206	0.206	0.206	0.206	40	0.207	0.207	0.207	0.207
Hornblendite (HBL)																										
S=6	Avg	3268	7.294	7.131	7.032	6.853	3272	7.306	7.120	7.002	6.788	3276	7.319	7.111	6.974	6.722	3280	7.331	7.103	6.945	6.657	3284	7.344	7.094	6.917	6.591
R=2	S.D.	1	0.036	0.036	0.036	0.036	1	0.041	0.041	0.041	0.041	1	0.047	0.047	0.047	0.047	1	0.052	0.052	0.052	0.052	1	0.057	0.057	0.057	0.057
Pyroxenite (PYX)																										
S=33	Avg	3288	7.908	7.745	7.646	7.468	3292	7.925	7.739	7.622	7.407	3296	7.942	7.735	7.598	7.346	3300	7.960	7.731	7.574	7.285	3304	7.977	7.728	7.550	7.224
R=11	S.D.	28	0.089	0.089	0.089	0.089	28	0.090	0.090	0.090	0.090	28	0.092	0.092	0.092	0.092	28	0.094	0.094	0.094	0.094	28	0.096	0.096	0.096	0.096
Dunite (DUN)																										
S=51	Avg	3324	8.385	8.222	8.124	7.945	3328	8.393	8.207	8.090	7.875	3331	8.401	8.193	8.056	7.804	3335	8.409	8.180	8.023	7.734	3339	8.416	8.167	7.990	7.664
R=17	S.D.	14	0.142	0.142	0.142	0.142	14	0.155	0.155	0.155	0.155	14	0.169	0.169	0.169	0.169	14	0.184	0.184	0.184	0.184	14	0.199	0.199	0.199	0.199

Densities in kg/m3 and velocities in km/s. Avg, average; S.D., standard deviation.

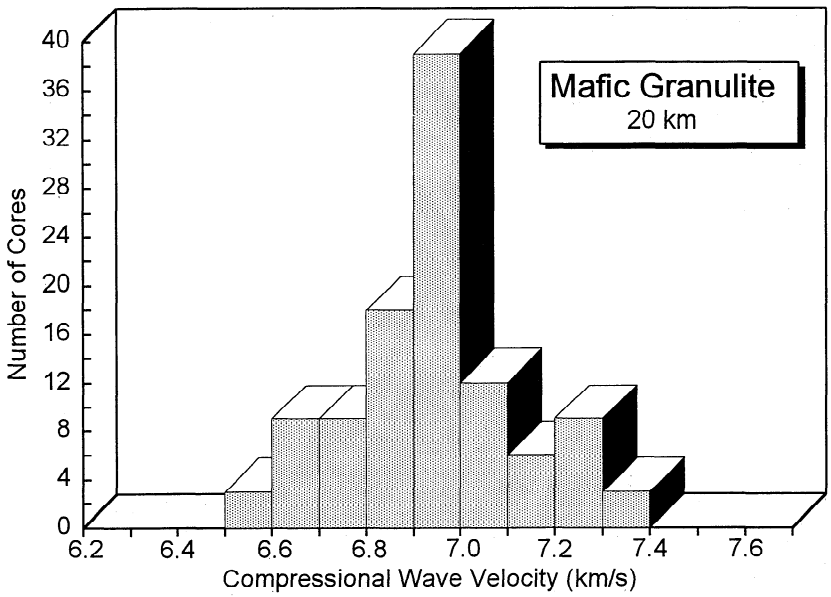

Figure 10. Mafic granulite velocities at pressures corresponding to 20 km depth.

sion becomes important in laboratory velocity measurements. Velocities are commonly calculated from transit times measured at elevated pressures and core lengths measured at atmospheric pressure. At high pressures, core lengths change due to sample compression. Velocities reported in the literature usually do not take this shortening into account, resulting in velocities which are high, by as much as 0.05 km/s [*Birch*, 1960]. These corrections, which have been applied to the data of Table 4, were determined from compressibilities calculated from velocity measurements and an iterative technique first described

Table 5. Average Compressional Wave Anisotropies and Standard Deviations

Rock Catagory	5 km	15 km	25 km	35 km
Granite-granodiorite	1.5 ± 1.0	1.3 ± 1.0	1.3 ± 0.9	1.3 ± 1.0
Diorite	1.3 ± 0.8	1.2 ± 0.8	1.1 ± 0.6	1.1 ± 0.6
Gabbro-norite-troctolite	2.0 ± 1.6	1.9 ± 1.5	1.9 ± 1.4	1.9 ± 1.4
Andesite	1.1 ± 0.7	1.0 ± 0.6	0.9 ± 0.5	0.9 ± 0.5
Basalt	1.7 ± 1.3	1.4 ± 1.1	1.3 ± 1.0	1.3 ± 1.0
Diabase	0.8 ± 0.8	0.7 ± 0.7	0.7 ± 0.6	0.7 ± 0.6
Zeolite facies basalt	0.9 ± 0.8	0.7 ± 0.6	0.7 ± 0.6	0.8 ± 0.6
Prehnite-pumpellyite facies basalt	3.2 ± 2.9	3.0 ± 2.9	2.9 ± 0.8	2.9 ± 2.7
Greenschist facies basalt	5.2 ± 4.2	4.5 ± 3.9	4.2 ± 3.7	4.1 ± 3.5
Slate	21.2 ± 6.4	19.3 ± 6.2	18.1 ± 6.1	17.2 ± 6.0
Metagraywacke	4.8 ± 3.5	4.1 ± 3.1	3.6 ± 2.5	3.3 ± 2.1
Phyllite	12.4 ± 7.7	10.6 ± 6.2	9.9 ± 5.6	9.5 ± 5.2
Marble	5.0 ± 3.0	4.6 ± 3.0	4.6 ± 2.9	4.6 ± 2.9
Felsic granulite	2.5 ± 1.5	2.4 ± 1.5	2.5 ± 1.6	2.5 ± 1.6
Mafic granulite	3.7 ± 2.8	3.3 ± 2.7	3.3 ± 2.6	3.3 ± 2.6
Mafic garnet granulite	5.7 ± 4.7	5.2 ± 4.3	4.9 ± 4.2	4.7 ± 4.2
Paragranulite	4.9 ± 4.8	4.8 ± 4.3	4.7 ± 4.1	4.7 ± 3.9
Anorthositic granulite	2.9 ± 1.8	2.8 ± 1.7	2.7 ± 1.8	2.8 ± 1.9
Amphibolite	10.2 ± 4.4	9.7 ± 4.2	9.4 ± 4.1	9.3 ± 4.1
Mica quartz schist	16.0 ± 8.7	14.0 ± 8.1	13.4 ± 8.0	13.0 ± 7.8
Granite gneiss	5.2 ± 4.0	4.2 ± 3.6	3.8 ± 3.5	3.9 ± 3.5
Tonalitic gneiss	9.7 ± 6.1	8.9 ± 5.7	8.5 ± 5.5	8.3 ± 5.3
Anorthosite	3.7 ± 2.1	3.4 ± 2.1	3.4 ± 2.1	3.4 ± 2.2
Eclogite	2.2 ± 1.1	1.9 ± 0.9	1.8 ± 0.9	1.9 ± 0.8
Dunite	8.1 ± 3.9	8.1 ± 3.9	8.0 ± 3.9	8.0 ± 3.9
Serpentinite	4.5 ± 1.6	4.4 ± 1.6	4.3 ± 1.6	4.2 ±1.6
Pyroxenite	3.6 ± 2.1	3.4 ± 1.8	3.4 ± 1.7	3.3 ± 1.6
Hornblendite	4.3 ± 1.3	3.7 ± 0.8	3.6 ± 0.9	3.7 ± 0.9
Quartzite	2.4 ± 0.8	2.1 ± 0.8	1.9 ± 0.9	1.9 ± 0.9

In percent.

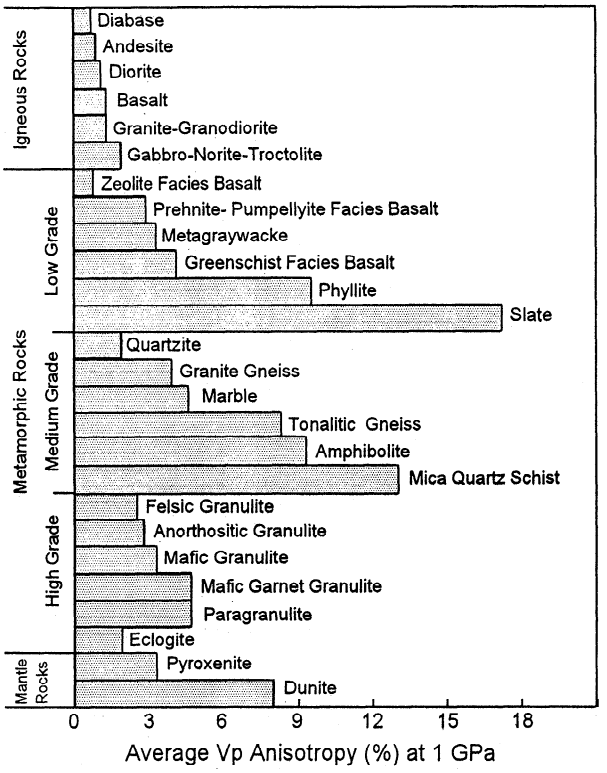

Figure 11. Average anisotropies, 100 $(V_{max}-V_{min})/V_{ave}$, at pressures corresponding to 35 km depth.

by *Christensen and Shaw* [1970]. The densities in Table 4 have also been corrected for compression. For convenience in comparing the laboratory velocities with field velocities, pressures have been converted to crustal depths at 5-km intervals, using a mean crustal density of 2830 kg/m^3.

With the exception of a few granites and basalts, velocities for each rock were measured in three directions from cores taken in mutually perpendicular directions. To a first approximation, simple averages of velocities in three directions give reasonable velocities for isotropic mineral aggregates [*Birch*, 1961]. Average anisotropies and standard deviations are given at four depth intervals in Table 5. The change in anisotropy with depth is minimal for most rock types. The origin of the anisotropies is preferred mineral orientation.

Compressional wave anisotropies at 1 GPa, corresponding to approximately 35 km depth, are shown in Figure 11 for several of the rocks of Table 4. The igneous rocks are to a first approximation isotropic, whereas many of the metamorphic rocks show significant anisotropy. Anisotropy is a particularly important parameter in the low-grade pelitic rocks, reaching average values of 9.5% in phyllite and 17.2% in slate. For the medium-grade metamorphic rocks, tonalitic gneiss, amphibolite and mica quartz schist have average anisotropies of 8.3%, 9.3%, and 13.0%, respectively. These values are all higher than the 8.0% average of mantle dunite. Low velocities correspond to propagation normal to cleavage, foliation or banding [*Christensen*, 1965]. The high grade granulite and eclogite facies rock are relatively low in anisotropy. Thus seismic anisotropy is likely to be a more significant property of upper and midcrustal regions than the lower crust. This is illustrated for mafic rocks in Figure 11 by following the change in anisotropy accompanying progressive metamorphism of basalt. Anisotropy increases from the zeolite facies through the prehnite pumpellyite facies and greenschist facies to a maximum value at amphibolite facies conditions and then decreases in mafic granulites and eclogites.

Crustal temperature is an important parameter bearing on the interpretation of seismic velocities. Temperature-depth models have been calculated by several authors for three heat flow provinces originally defined by *Roy et al.* [1968], the Sierra Nevada, eastern United States, and Basin and Range, corre-

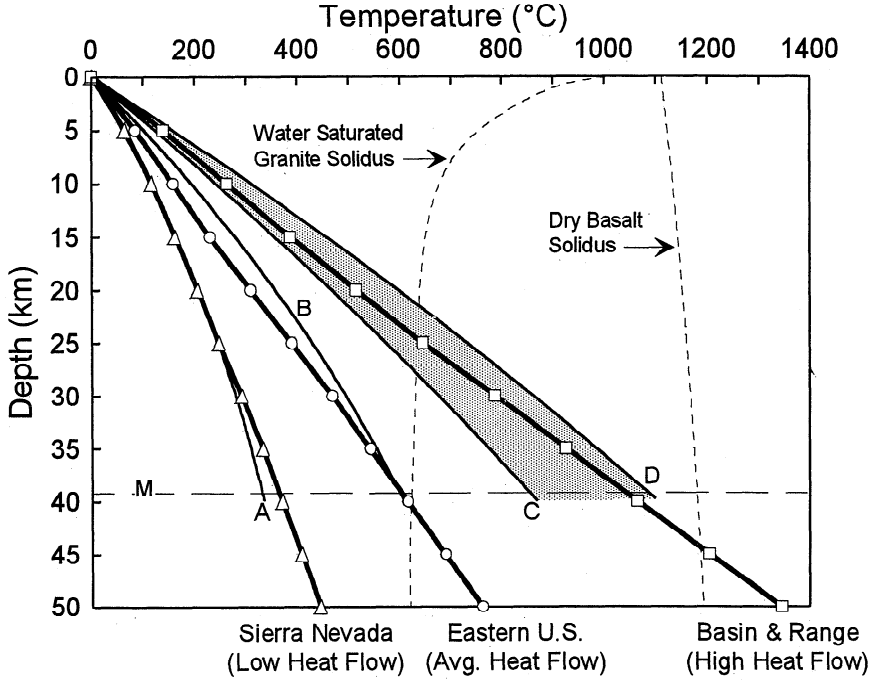

Figure 12. Temperature-depth curves for three heat flow provinces after *Blackwell* [1971] (triangles, circles, and squares) and *Lachenbruch and Sass* [1977] (curves A, B, C, and D). Average crustal thickness is shown as the dashed line "M".

Table 6. Temperature Coefficients

Rock	$\partial Vp/\partial T$ km s^{-1} °C^{-1}
Granite - granodiorite, granitic gneiss, tonalitic gneiss	-0.39×10^{-3}
Gabbro - norite - troctolite	-0.57×10^{-3}
Basalt, metabasalt	-0.39×10^{-3}
Slate, phyllite, quartz mica schist	-0.40×10^{-3}
Mafic granulite, mafic garnet granulite	-0.52×10^{-3}
Felsic granulite, paragranulite	-0.49×10^{-3}
Amphibolite	-0.55×10^{-3}
Anorthosite	-0.41×10^{-3}
Dunite, pyroxenite, hornblendite	-0.56×10^{-3}
Eclogite	-0.53×10^{-3}
Serpentinite	-0.68×10^{-3}
Quartzite	-0.54×10^{-3}
Marble	-0.41×10^{-3}

From Christensen [1979, also unpublished data, 1980].

sponding to low, average, and high heat flow, respectively. To illustrate the range of possible crustal temperatures, the preferred models of *Blackwell* [1971] and *Lachenbruch and Sass* [1977] are compared in Figure 12. These studies and more recent continental heat flow summaries [e.g., *Morgan and Gosnold*, 1989] conclude that temperature differences between the three provinces are much larger than temperature uncertainties introduced by different modeling assumptions. The temperatures in Table 4 at 5-km depth intervals are from *Blackwell* [1971].

In comparison with measurements at elevated pressures, the influence of temperature on seismic velocities has received only limited attention. To avoid formation of cracks during the heating of rocks, which leads to irreversible decreases in velocity, it is necessary to raise the pressure a few hundred megapascals before heating [*Birch*, 1943]. Temperature coefficients obtained at elevated pressures show a fairly narrow range of values for most common rocks [e.g., *Fielitz*, 1971; *Kern*, 1978; *Christensen*, 1979]. Values of $(\partial Vp/\partial T)_p$ used to obtain velocities for the three heat flow provinces of Table 4 are summarized in Table 6. These values were applied to the velocity-pressure data obtained at room temperature.

The importance of applying temperature corrections to laboratory velocity data prior to making comparisons with continental crustal seismic velocities is illustrated in Figure 13 for average granite/granodiorite and average mafic granulite. The corrected curves for the three heat flow provinces increase in velocity until depths of 10 to 15 km are reached, where grain boundary cracks are closed, and decrease at greater depths. For geothermal gradients different from those used in Table 4, it is possible to arrive at reasonable velocity values by simple extrapolation. For velocities along the high heat flow geotherm, the reader should be cautioned that partial melting, especially in the more silicic water saturated rocks, may cause significant departures from the velocities in Table 4. Also, above approximately 500°C, velocities in quartz-rich rocks are likely to be affected by the quartz α-β transition [e.g., *Fielitz*, 1971].

Average velocities and standard deviations for the major rock types, arranged in order of increasing velocity at pressures corresponding to 20 km depth, are illustrated in Figure 14. Velocities under 6.0 km/s are limited to serpentinite, metagraywacke, andesite, and basalt. A large variety of rocks have average velocities falling between 6.0 km/s and 6.5 km/s, including granite, diorite, slate, phyllite, zeolite facies basalt, prehnite-pumpellyite facies basalt, amphibolite facies granitic gneiss, tonalitic gneiss and schist, and felsic granulite facies rocks. With the exception of marble and anorthosite, rocks with velocities between 6.5 km/s and 7.0 km/s are mafic in composition. These include diabase, greenschist facies basalt, amphibolite and mafic granulite. Rocks with average velocities between 7.0 km/s and 7.5 km/s include gabbro, hornblendite, and mafic garnet granulite. In the classification adopted for Table 4, the distinction between mafic garnet granulite and mafic granulite is based solely on the presence or absence of garnet. Velocities above 7.5 km/s are limited to pryoxenite, eclogite, and dunite. Lithologies with relatively large standard deviations (e.g., metagraywacke, quartz mica schist, and the low-grade metabasalts) have extremely variable mineralogies and are sometimes significantly anisotropic. The wide range in velocities in basalt is also a consequence of glass content, porosity, often in the form of small vesicles which do not close at elevated pressures, and secondary alteration. As earlier observed by *Birch* [1961], diabase is significantly lower in velocity than gabbro. This is likely related to mineralogical differences, since many of the gabbros contain abundant high-velocity olivine, whereas the diabases in this compilation are usually olivine-free.

The order of increasing velocity illustrated in Figure 14 shows that velocity is not simply a function of metamorphic grade. This is demonstrated in Figure 15 where histograms of rock velocities for the major metamorphic facies are compared with velocities at 20 km depth for plutonic igneous rocks ranging in composition from granite to gabbro and ultramafic rocks. Figure 15 illustrates that crustal velocities in the range of 6.0 to 7.5 km/s can be matched with low-, medium-, and high-grade metamorphic rocks, as well as common igneous rocks. The narrow range of high velocities observed in the eclogite facies rocks is due to the limited compositional range generally found

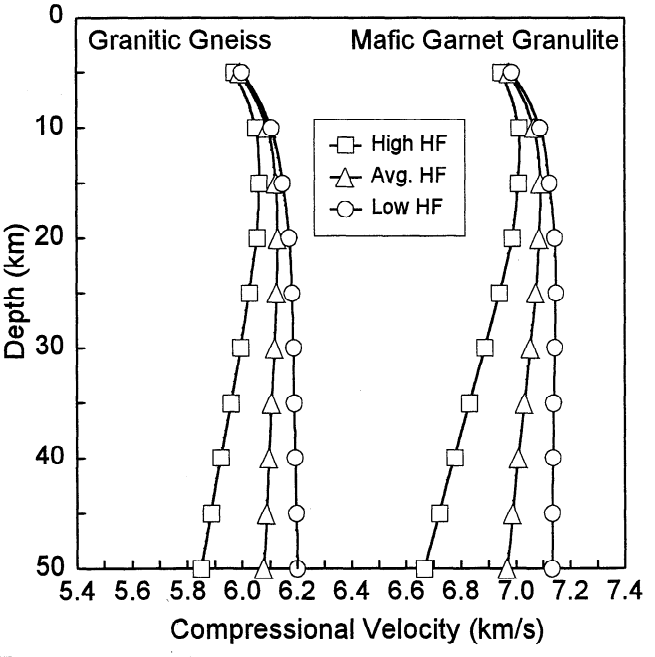

Figure 13. Velocity versus depth and heat flow province for average granite/granodiorite and mafic garnet granulite . For temperatures, see Table 4.

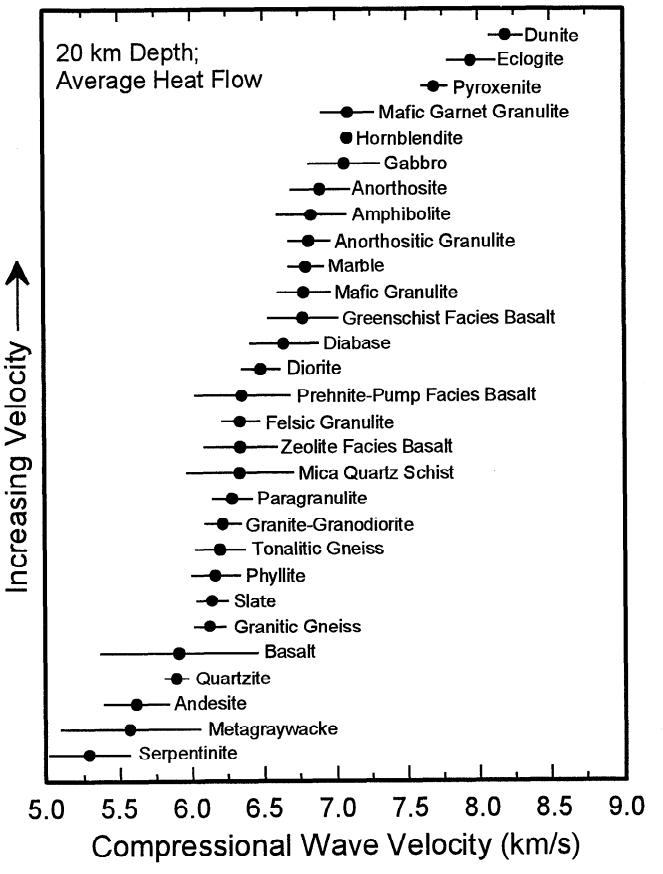

Figure 14. Average compressional wave velocities and standard deviations at 20 km depth and 309°C (average heat flow) for major rock types.

in eclogite facies mineral assemblages. The wide range of velocities observed for the ultramafic rocks is due to variable serpentinization. Serpentinite has the lowest velocities, whereas dunites with velocities above 8.3 km/s are virtually serpentine-free.

Velocity-Density Relationships

Correlations between compressional wave velocity and density are important because they allow estimates of crustal density to be made for gravity modeling from seismic refraction velocities and, conversely, because rock densities can be used to predict seismic velocities. Examples of velocity-density relations in wide use include the Nafe-Drake curve [*Nafe and Drake*, 1957], *Birch's* [1961] law relating velocity, density, and mean atomic weight, and regression line solutions for oceanic rocks [*Christensen and Salisbury*, 1975]. In Figure 16, average velocities for our 29 rock categories at a depth of 20 km and a temperature of 309°C, corresponding to an average geotherm, are plotted against densities.

In Table 7, the parameters of least squares solutions of the forms $\rho = a + bVp$ and $Vp = a + b\rho$ are given at several depths. Velocities have been corrected for temperatures corresponding to the average heat flow temperature values of Table 4. We have chosen two sets of solutions, one set for all rock types included in Table 4 and a subset shown as solid circles in Figure 16 with a least squares straight-line fit, which does not include monomineralic rocks and basalt and andesite. We prefer the latter set of solutions, since it is unlikely that the unmetamorphosed volcanic rocks or the monomineralic rocks are abundant crustal lithologies at depth. Coefficients of determinations are high (> 90%) for this subset. The monomineralic rocks quartzite, serpentinite, and hornblendite have relatively

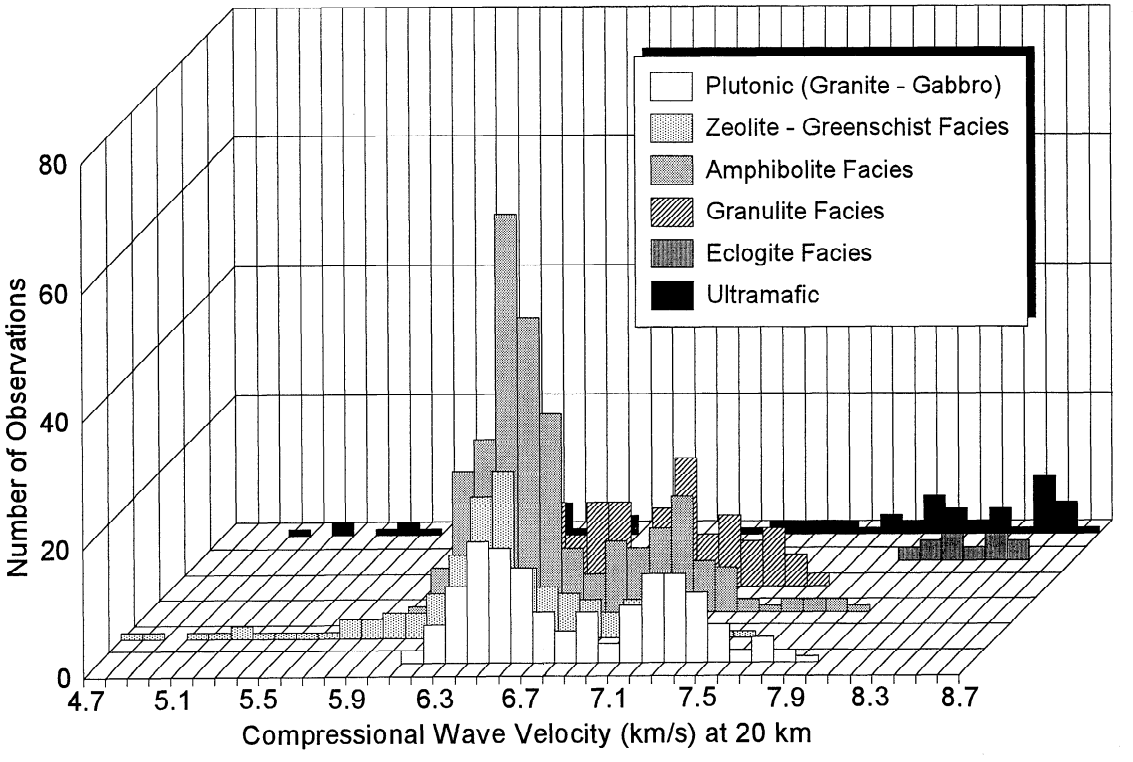

Figure 15. Velocities at 20 km depth for plutonic igneous rocks ranging in composition from granite to gabbro, metamorphic rocks of various facies, and serpentinized to unaltered ultramafic rocks. Note that rocks of all the major metamorphic facies, plutonic igneous rocks, and partially serpentinized peridotites have velocities within the commonly observed crustal velocities of 6.0 km/s to 7.5 km/s.

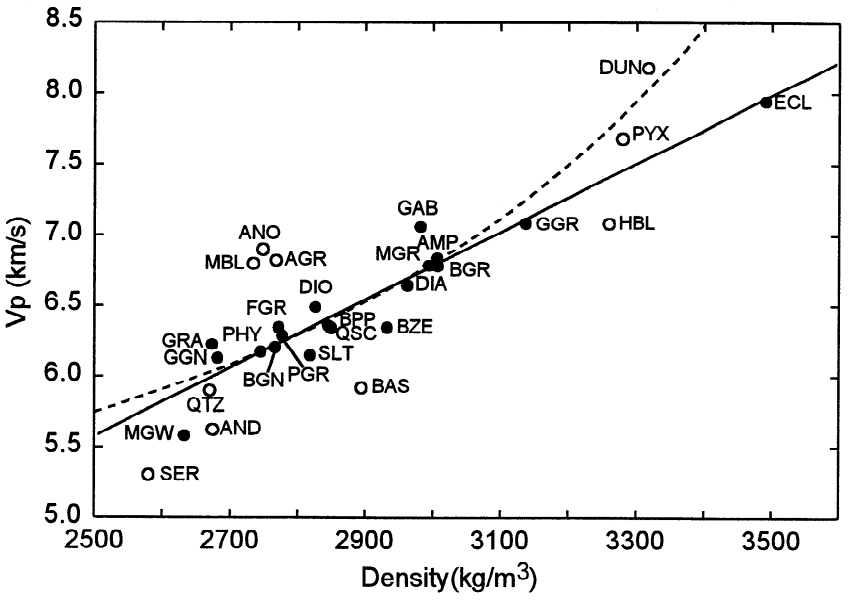

Figure 16. Average velocity versus average density for a variety of rock types at a pressure equivalent to 20 km depth and 309°C. Rock abbreviations are given in Table 4. Regression line parameters at various depths are given in Tables 7 and 8. The nonlinear solutions are recommended for crust-mantle calculations (see text).

low velocities for their densities, whereas the anorthosites, marble, pyroxenite, and dunite have high velocities. The polymineralic lithologies functionally average these high and low velocities and densities of the mineral constituents, so that bulk velocities and densities produce a better linear fit.

Note that the linear solution in Figure 16 for the crustal rocks departs sharply for the mantle rocks pyroxenite (PYX) and dunite (DUN). Thus the linear solutions of Table 7 are not recommended for comparing crust and peridotite mantle. For velocity-density solutions applicable to crust-mantle sections, the data have been fit to several hundred nonlinear equations. The data set which we have selected for these regression line fits includes the mantle rocks dunite and pyroxenite and the polymineralic crustal rocks. We assume that the upper mantle is predominantly peridotite, and thus we have removed eclogite data. The best correlations between density and velocity for relatively simple equations are of the form $\rho = a + b/Vp$ for calculating density from velocity and $Vp^{-1} = a + b\rho^3$ for obtaining velocity from density. The parameters of these curve fits are given in Table 8 at various depths. The 20-km solution for the latter equation is shown as the dashed curve in Figure 16. The solutions in Table 8 are recommended for use in gravity calculations of crust-mantle density contrasts.

Seismic Constraints on Crustal Composition

The compilations presented in the previous sections provide a new basis for generalizations on continental petrology and

Table 7. Linear Velocity-Density Regression Line Parameters

	$\rho = a + bVp$				$Vp = a + b\rho$			
Depth, km	a, kg m^{-3}	b, kg m^{-3}/km s^{-1}	$S(\rho, Vp)$, kg m^{-3}	r^2, %	a, km s^{-1}	b, km s^{-1}/kg m^{-3}	$S(Vp, \rho)$, km s^{-1}	r^2, %
				All Rocks				
10	989.3	289.1	116.3	75	-0.924	0.00259	0.348	75
20	947.3	296.6	113.3	76	-0.836	0.00256	0.333	76
30	946.6	299.7	112.5	76	-0.802	0.00252	0.326	76
40	964.5	300.5	113.3	75	-0.764	0.00249	0.326	75
50	1078.3	299.0	120.3	71	-0.775	0.00238	0.339	71
				All Rocks Except Volcanic Rocks and Monomineralic Rocks				
10	540.6	360.1	70.2	88	-0.566	0.00245	0.183	88
20	444.1	375.4	62.8	91	-0.454	0.00241	0.159	91
30	381.2	388.0	57.8	92	-0.377	0.00237	0.143	92
40	333.4	398.8	53.8	93	-0.318	0.00232	0.130	93
50	257.1	431.4	49.1	94	-0.192	0.00218	0.110	94

Vp is compressional wave velocity; ρ, density; $S(\rho, Vp)$, standard error of estimate of ρ on Vp; $S(Vp, \rho)$, standard error of estimate of Vp on ρ; r^2, coefficient of determination.

Table 8. Nonlinear Velocity-Density Regression Line Parameters

	$\rho = a + b/Vp$				$Vp^{-1} = a + b\rho^3$			
Depth, km	a, kg m^{-3}	b, kg m^{-3}/km s^{-1}	$S(\rho, Vp)$, kg m^{-3}	r^2, %	a, km/s^{-1}	b -	$S(Vp, \rho)$, km s^{-1}	r^2, %
10	4929	-13294	69.30	87	0.2124	-2.4315×10^{-12}	0.19	91
20	5055	-14094	62.20	90	0.2110	-2.3691×10^{-12}	0.17	92
30	5141	-14539	57.36	91	0.2115	-2.3387×10^{-12}	0.15	93
40	5212	-14863	53.63	92	0.2123	-2.3155×10^{-12}	0.14	94
50	5281	-15174	50.51	93	0.2130	-2.2884×10^{-12}	0.13	95

Vp is compressional wave velocity; ρ, density; $S(\rho, Vp)$, standard error of estimate of ρ on *Vp*; $S(Vp, \rho)$, standard error of estimate of *Vp* on ρ; r^2, coefficient of determination.

chemistry. In Figure 17, average velocity-depth curves for a variety of major igneous and metamorphic rock types are superimposed on our average crustal velocity model. We have divided the rock types into five major groups (monomineralic, igneous, and low-, medium-, and high-grade metamorphic rocks). All velocity-depth curves are at temperatures corresponding to the average geotherm of Table 4. It should be noted that in all five diagrams, velocities for the upper 5 km are not shown, since at these shallow depths, velocities are often lowered significantly by cracks.

Monomineralic Rocks

The monomineralic rock averages are perhaps most useful in understanding the contributions of selected minerals to rock velocities. Velocities of serpentinite and quartzite fall significantly below middle and lower crustal velocities, whereas velocities of pyroxenite and dunite are much higher than even the fastest lower crustal velocities. Various combinations of anorthosite, hornblendite, and pyroxenite can readily be equated to observed lower crustal velocities, suggesting that plagioclase, amphibole, and pyroxene are abundant lower crustal minerals. Note also the relatively high velocities of marble which match our weighted average crustal velocities at 25 to 30 km depths. On the basis of surface exposures of medium- to high-grade metamorphic terranes, marble does not appear to be a particularly abundant midcrustal lithology. Calc-silicates are, however, common suggesting a breakdown of carbonates with loss of CO_2 and the production of silicate minerals.

Igneous Rocks

Early seismic studies often interpreted crustal seismic data in terms of igneous lithologies. Figure 17 shows how an igneous crustal model is in agreement with our average crustal velocity-depth curve. Uppermost crustal velocities of this model match either an assemblage of volcanic rocks or fractured plutonic rocks. At greater depths the velocities can be simply explained by a gradual change from granite/granodiorite through diorite at 20 km to gabbro at 40 km. Diabase dikes have velocities equivalent to average crustal velocities at 25 km, and anorthosite velocities are similar to crustal velocities at 35 km.

Metamorphic Rocks

The concept of a crustal section consisting of simple igneous lithologies has been under attack for many years as Earth scientists gradually turned to models consisting of metamorphic assemblages [e.g., *Christensen*, 1965; *Ringwood and Green*, 1966]. In particular, there has been almost universal agreement that the lower crust in stable platforms must contain high-grade metamorphic rocks in the granulite and/or eclogite facies. However, the specific chemistry of these rocks has been widely debated, with several studies concluding that the lower crust consists on the average of rocks of intermediate rather than mafic silica composition [e.g., *Ringwood and Green*, 1966; *Smithson et al.*, 1981].

Average upper crustal velocities are in the range of many metamorphic rock types. Observed velocities within the top 15 km of the crust match laboratory velocities of slates and phyllites and interlayered metagraywacke and low-grade metabasalt. Surface exposures of similar assemblages are common in many forearc regions, such as the Franciscan of California [e.g., *Hamilton and Meyers*, 1966] or the Chugach of Alaska [e.g., *Plafker et al.*, 1989], where processes involving accretion have been active along continental margins. In older shields and many orogenic regions, where erosion has exposed rocks consisting of granitic gneiss or an assemblage of quartzite, quartz mica schist, tonalitic gneiss, and minor amphibolite, upper crustal velocities match velocities of these medium-grade metamorphic rocks. Note that the high-grade metamorphic rocks have velocities higher than average upper crustal velocities, which is consistent with the rare occurrences of granulite and eclogite facies rocks in surface exposures.

At depths between 15 km and 30 km, average crustal velocities increase from approximately 6.3 km/s to 6.7 km/s. Within many crustal sections, this is undoubtedly a depth range where metamorphic grade increases from amphibolite facies to granulite facies. Progressive metamorphism is likely responsible for some velocity increase over this depth range. However, the velocity comparisons in Figure 17 also show that this middle crustal region must also change composition gradually to higher percentages of mafic mineral assemblages. At greater depths (from 30 km to 50 km), velocities can be simply explained as originating from a predominately mafic lower crust, with a lowermost section of mafic garnet granulite. Alternatively, the lower crust could contain felsic granulite facies rocks if mafic eclogites are present in similar proportions. However, we wish to emphasize that on the basis of our field and laboratory comparisons, the bulk of the lower continental crust is likely of mafic composition.

Estimates of crustal composition have been derived from a wide variety of observations, including average chemistries of crystalline rocks from surface exposures [e.g., *Clarke and*

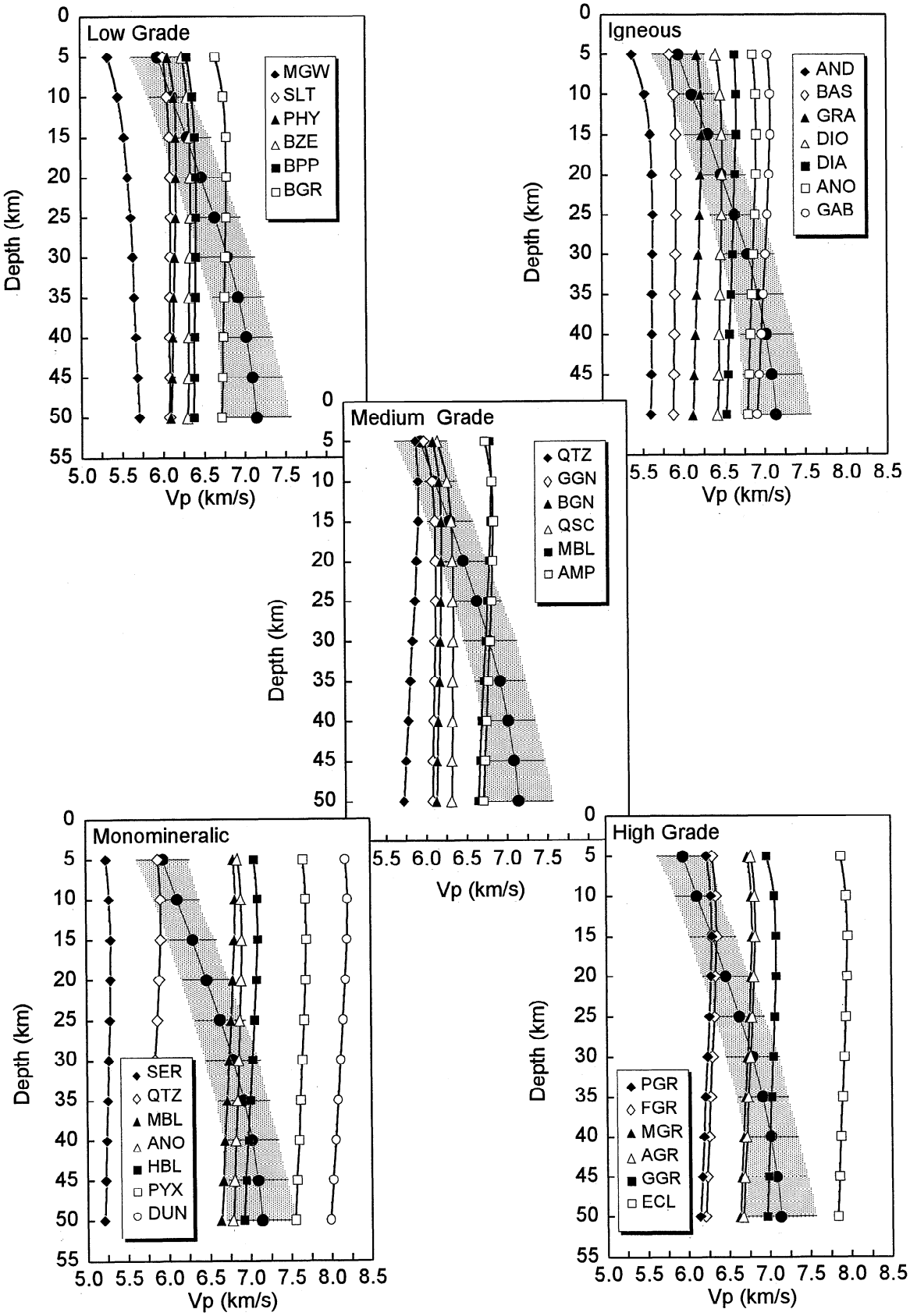

Figure 17. Average continental velocity structure compared to average laboratory measured velocities in major rock types. Rock abbreviations are given in Table 4.

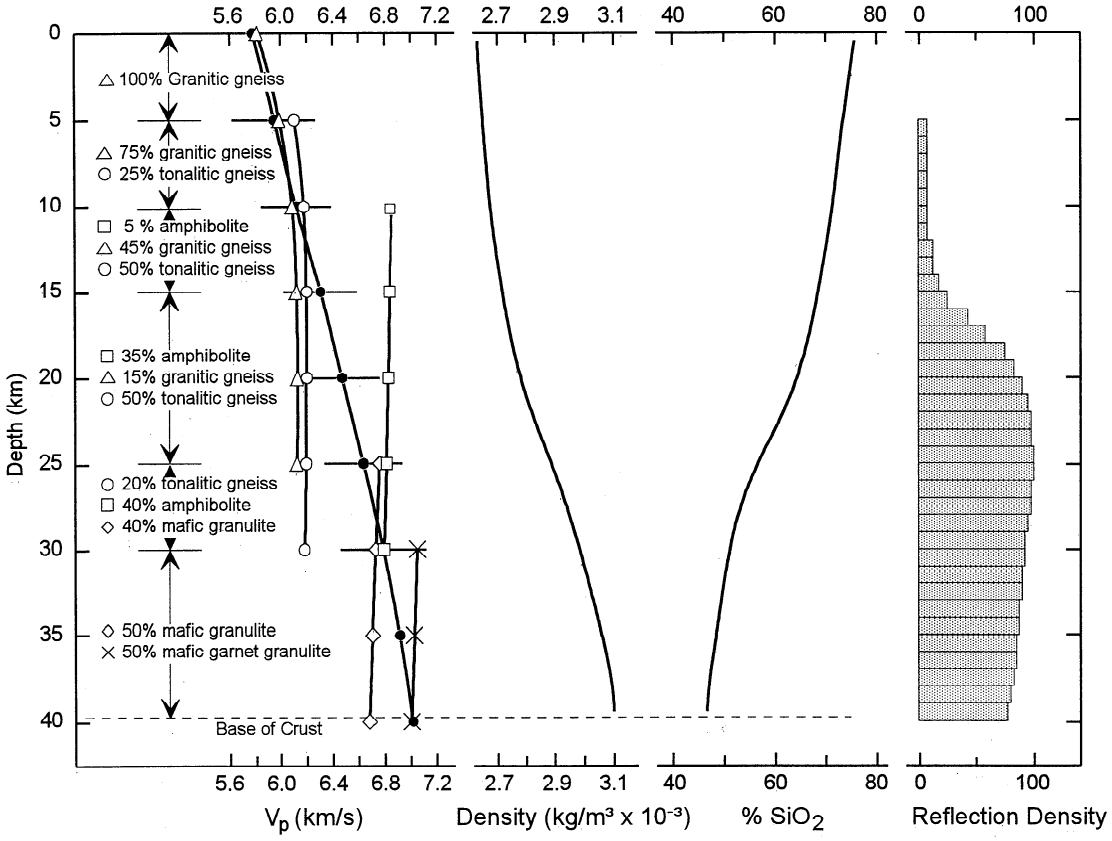

Figure 18. A model for average crustal petrology versus depth consistent with our average velocity depth profile (solid circles) and velocity depth curves for common rock types (open symbols). Variations of density and SiO_2 content with depth are from rock percentages shown on the left. Histograms of reflection densities are normalized with reflections originating from metamorphic layering.

Washington, 1924], comparisons of crustal seismic velocity profiles with laboratory measurements [e.g., *Birch*, 1958; *Fountain and Christensen*, 1989], estimates of mean crustal velocity [*Smithson et al.*, 1981], Poisson's ratios of the crust [e.g., *Christensen and Fountain*, 1975; *Holbrook et al.*, 1992], studies of xenoliths from volcanic and kimberlitic eruptions [e.g., *McGetchin and Silver*, 1972; *Kay and Kay*, 1981], and models of crustal structure based on the geology of exposed crustal sections [e.g., *Schmidt and Wood*, 1976; *Fountain and Salisbury*, 1981; *Miller and Christensen*, 1994]. Each of these methods has provided important constraints on the chemical and mineralogical compositions of the crust; however, each approach has serious limitations due to a wide variety of assumptions. In the following discussion, we present a model for crustal petrology and chemistry based on comparisons of our crustal velocity-depth profile with velocities of major crustal lithologies. This approach perhaps most closely follows an early geochemical estimate of bulk crustal composition by *Pakiser and Robinson* [1966], in that we are dealing with observed average velocity structure and laboratory measured velocities. Pakiser and Robinson divided the crust underlying the United States into an upper granitic layer and a lower basaltic layer. Volumes of these two layers were estimated from seismic data, and crustal chemistry was calculated from average chemical analyses of granitic and basaltic rocks.

In Figure 18, we have modeled the petrology of the average continental crust based on relatively simple metamorphic rock assemblages possessing velocities similar to our average crustal velocity-depth curve. Our estimate of crustal petrology is based on a selection of rock assemblages which are commonly observed in exposures of crustal sections. For example, the association of granitic gneiss, tonalitic gneiss, and amphibolite is common in many metamorphic terranes and their combined seismic properties are similar to those of many midcrustal regions [*Christensen*, 1989]. Also, crustal sections originating from greater depths often contain abundant mafic granulite [e.g., *Percival et al.*, 1992]. Our weighted average crustal velocity profile is shown in Figure 18 as solid circles with horizontal lines representing ± one standard deviation. Velocity-depth curves for granitic gneiss, tonalitic gneiss, amphibolite, mafic granulite, and mafic garnet granulite are superimposed on the crustal profile. Percentages of these rock types consistent with average crustal velocities over selected depth intervals are shown on the left of Figure 18.

This model assumes that the upper crustal section contains granitic gneiss which becomes increasingly tonalitic at depth. In addition, amphibolite becomes abundant at midcrustal depths. The region between 25 km and 30 km marks a transition from amphibolite facies rocks to granulite facies assemblages. At greater depths, garnet becomes increasingly abundant and mafic garnet granulite is the dominant rock type immediately above the Mohorovicic discontinuity. The crustal density of this model increases from 2660 kg/m^3 at the surface to 3100 kg/m^3 at the base of the crust. Also shown in Figure 18

Table 9. Bulk Crustal Chemical Composition

Oxide, wt %	*Clarke* [1924]	*Pakiser and Robinson* [1966]	*Taylor and McLennan* [1981]	*Weaver and Tarney* [1984]	This Work*
SiO_2	59.0	57.9	58.0	63.2	61.7
TiO_2	1.0	1.2	0.8	0.6	0.9
Al_2O_3	15.2	15.2	18.0	16.1	14.7
Fe_2O_3	3.1	2.3	...	...	1.9
FeO	3.7	5.5	7.5	4.9	5.1
MgO	3.5	5.3	3.5	2.8	3.1
CaO	5.1	7.1	7.5	4.7	5.7
MnO	0.1	0.2	0.1	0.1	0.1
Na_2O	3.7	3.0	3.5	4.2	3.6
K_2O	3.1	2.1	1.5	2.1	2.1
P_2O_5	0.3	0.3	...	0.2	0.2
H_2O	1.7	...	...	...	0.8

*Bulk continental crust from average crustal velocity-depth curve (Figure 18).

is the variation in weight percent of SiO_2 with depth, calculated from average chemical analyses of the rock suites at 5-km intervals.

A histogram of reflection density [*Meissner*, 1986] for our crustal model, normalized according to the maximum number of reflections per kilometer depth, is shown in Figure 18. The reflection histogram is based on synthetic modeling with horizontal layering. Reflection coefficients were determined from the rock velocities and densities presented in Table 4. The initiation of major reflections at midcrustal depths originates from the large contrasts in acoustic impedance of amphibolite with granitic gneiss and tonalitic gneiss. Seismic modeling of reflectivity from a similar sequence of rocks, obtained from a continuous drill core in the southern Appalachian Piedmont, substantiates the significant reflectivity of this assemblage [*Christensen*, 1989]. At deeper levels, garnet-rich layers, with high densities and velocities, are likely to be significant reflectors.

We have calculated an average chemistry of the continental crust from the volume percentages of the various rock types in our model (Figure 18) and their average chemical compositions. Because most models have assumed that the upper crust is "granitic" and overlies a "mafic" lower crust, our average (Table 9) is quite similar to many previous estimates of crustal chemistry. Our basic approach in obtaining average chemistry is unique, however, in that we have identified likely metamorphic rock assemblages at various crustal levels based on comparisons of our average crustal velocity column with the new database on rock velocities. The bulk continental chemistry presented in Table 9 is probably a reasonable approximation for many crustal sections. Regional variations are almost certainly important but poorly understood at this time.

Implications for Crustal Evolution

The results presented in this paper have broad implications for models of crustal evolution. Our histogram of crustal thickness (Figure 2) shows that very little continental crust is either thicker than 58 km or thinner than 24 km. Nearly all continental crust with a thickness outside the 24-56 km range is late Cenozoic in age (either highly extended crust or thickened orogenic crust). This observation implies that very thick crust, such as in Tibet and the Andes, will not remain thick but will evolve toward crust with a more typical thickness of about 40 km. The primary processes involved are probably isostatic uplift and erosion and the lateral flow of warm, rheologically weak middle and lower crustal rocks [*England and Houseman*, 1989]. An additional crustal process is the delamination of the lower crust beneath thick orogens [*Kay and Kay*, 1991], as is hypothesized to be occurring beneath the Alps based on seismic images.

Continental crust that is thinner than 24 km, whether it has been highly extended or formed at an active margin, will be underlain by a weak, thin lithosphere and is therefore likely to be subject to compressional collapse and thickening. Long-lived, stable crust, the Precambrian platforms and shields have cold, 40-km thick crust, with a mafic lower crust that is rheologically strong due to its lower silica content (Figure 18).

It is generally agreed that the rocks that constitute the Earth's crust originated from igneous processes associated with extraction of material from the mantle. The processes of crustal growth involve not only magmatic contributions from the mantle but also accretion of tectonic terranes, as well as crustal recycling, the latter resulting in negative growth. The ultimate fate of most newly formed crust is to become attached to old nuclei, which we have included in our compilation as shields and platforms.

The average tectonic columns of Figures 7 and 9 provide insight into the nature of the tectonic and magmatic processes required to evolve continental arcs and orogens into stable shield orogens and platforms. First, a comparison of the velocity structures of continental arcs with shields and platforms shows that they have similar lower crustal velocity profiles. Continental arcs, however, appear to have significantly higher velocities in their upper 20 km, suggesting that the upper sections of continental arcs must be modified by the intrusion of silicic magmas, or by the incorporation of metasedimentary rocks through a complex tectonic history, before being converted to shields and platforms. Second, the low velocities of orogens can be converted to shield and platform velocities by

the intrusion of a significant volume of mafic magma or simple isostatic uplift of approximately 5 km associated with surficial erosion. Such uplift is also required to satisfy crustal thickness observations, as mentioned above.

We have presented evidence that the lower crust of the continents is typically composed of mafic granulites with about 47% SiO_2 and that the silica content increases to greater than 70% in the upper crust (Figure 18). This observation is consistent with at least two hypotheses regarding the evolution of stable crust that the crust grows primarily either by the accretion of continental magmatic arcs or by the accretion of diverse geological terrains that undergo secondary differentiation soon after accretion [*Meissner and Mooney*, 1991]. The first model is consistent with our data. In the latter model, the lower crust is melted by heat provided by intruding mafic magmas, and differentiation produces granitic and dioritic plutons that move up into the upper and middle crust. This process of differentiation will also produce a mafic/ultramafic residuum at the base of the crust, and the ultramafic material will form a new, young Moho at a depth of about 40 km. We note that either of these processes, accretion of intact magmatic arcs or differentiation of diverse accreted terrains, predominantly involves magmatic processes to produce stable continental crust.

Summary and Conclusions

Any model of the continental crust must be consistent with three fundamental observations: (1) the seismic structure of the continental crust, (2) the petrology of surface exposures of crustal sections which have previously been buried to various depths, and (3) laboratory measurements of seismic velocity through the commonly observed lithologies of surface exposures. In this paper we have presented models for the seismic structure and composition of the continental crust based on a worldwide data set of seismic refraction profiles, as well as a comprehensive summary of compressional wave velocities as a function depth for a wide variety of continental igneous and metamorphic rocks.

The thickness and velocity structure of the crust are well correlated with tectonic province and reflect the processes that have formed and modified the crust. Shields and platforms have an average crustal thickness of 41.5 km, nearly equal to the global average. Extended crust has an average thickness of 30.5 km and a low average crustal velocity of 6.2 km/s. Rifts and orogens show a wide range of crustal thickness, 18-46 km and 30-72 km, respectively.

The available global seismic refraction data have a nonuniform geographic distribution, which results in a strong geographical bias in such quantities as average crustal thickness and average crustal velocity. In order to correct the nonuniform data distribution, we have calculated average crustal properties using a weighted average of five tectonic provinces: shields and platforms, orogens, extended crust, magmatic arcs, and rifts. Mean weighted values of crustal thickness, average crustal velocity, and *Pn* velocity are 41.0 km, 6.45 km/s, and 8.09 km/s, respectively.

Average velocities, densities, and standard deviations presented for 29 igneous and metamorphic rock types believed to be abundant in the continental crust show a wide range of velocities similar to the range reported in crustal refraction studies. Average upper crustal velocities match laboratory measured velocities of a variety of rocks, including granitic gneiss and interlayered assemblages of metagraywacke, slate, phyllite, and meta-basalt. In midcrustal regions, at depths of 10 km to 25 km, amphibolite facies rocks are likely to comprise the bulk of the crust. Within this region, there is a gradual change in composition from granitic gneiss and tonalitic gneiss to mafic mineral assemblages rich in amphibole. At depths greater than 30 km, the continental crust contains abundant granulite facies rocks of mafic composition. Observed velocity gradients in this region indicate that garnet content increases with depth.

Seismic anisotropy originating from preferred mineral orientation is likely to be an important property of upper and midcrustal regions. Maximum anisotropy is expected in upper crustal metamorphic terranes containing abundant slate and phyllite and deeper crustal sections of amphibolite and quartz mica schist. Presently, it is not possible to take into account the influence of anisotropy on our crustal averages since the presence of crustal anisotropy has only recently been documented [e.g., *Brocher and Christensen*, 1990] We look forward to the findings of future seismic field programs designed specifically to investigate the magnitude and symmetry of anisotropy at various crustal levels. These studies will not only reveal important information on crustal structure and deformation but will also add much to our understanding of crustal composition.

Crustal density for our model increases from 2660 kg/m^3 at the surface to 3100 kg/m^3 at 40 km. Average crustal density is 2835 kg/m^3. SiO_2 decreases with depth from over 70% in the upper 5 km of the crust to 47% at the Mohorovicic discontinuity. The average weight percent SiO_2 calculated from our crustal model is 61.8%, in good agreement with many previous estimates.

In the model presented in this paper, we have attempted to explain seismic velocity observations of the continental crust in terms of a petrologic model consistent with new laboratory velocity measurements on common continental rocks. The crustal model adopted was founded on simple petrologic observations based primarily on studies of deep exposures of continental crust, but to obtain information on the relative abundances of rocks at crustal depths it was necessary to compare the velocities with seismic structure. We stress that our model is only an average representation of crustal petrology and chemistry and variations from this average are certain. These variations in crustal composition are poorly understood at this time, but of prime importance in understanding continental crustal genesis and evolution.

Acknowledgments. The manuscript was greatly improved by the perceptive comments of George Thompson, Roy Johnson, Randy Keller, Bill Hinze, Tom Brocher, and Jill McCarthy. K. Wilcox, D. Kingma, W. Wepfer, and Jianping Xu provided valuable technical support for the experimental phase of this study. Financial support for the laboratory studies was provided by the Office of Naval Research and the National Science Foundation Continental Dynamics Program. The field compilation has been supported by the USGS Deep Continental Studies Program.

References

Allenby, R. J., and C. Schnetzler, United States crustal thickness, *Tectonophysics, 93*, 13-31, 1983.

Bamford, D., *Pn*-velocity anisotropy in a continental upper mantle, *Geophys. J. R.. Astron. Soc., 49*, 29-48, 1977.

Beloussov, V. V., N. I. Pavlenkova, and A. V. Egorkin, *Deep Structure of the Territory of the USSR*, 224 pp., Nauka, Moscow, 1991.

Birch, F., Elasticity of igneous rocks at high temperatures and pressures, *Geol. Soc. Am. Bull., 54*, 263-286, 1943.

Birch, F., Interpretation of the seismic structure of the crust in light

of experimental studies of wave velocities in rocks, in *Contributions in Geophysics in Honor of Beno Gutenberg*, edited by H. Benioff, pp. 158-170, Pergamon, New York, 1958.

Birch, F., The velocity of compressional waves in rocks to 10 kilobars, 1, *J. Geophys. Res.*, *65*, 1083-1102, 1960.

Birch, F., The velocity of compressional waves in rocks to 10 kilobars, 2, *J. Geophys. Res.*, *66*, 2199-2224, 1961.

Blackwell, D. D., The thermal structure of the continental crust, in *The Structure and Physical Properties of the Earth's Crust, Geophys. Monogr. Ser.*, vol. 14, edited by J. G. Heacock, pp. 169-184, AGU, Washington, D.C., 1971.

Braile, L. W., W. J. Hinze, R. R. B. von Frese, and G. R. Keller, Seismic properties of the crust and uppermost mantle of the conterminous United States and adjacent Canada, in Geophysical Framework of the Continental United States, edited by L. C. Pakiser and W. D. Mooney, *Mem. Geol. Soc. Am.*, *172*, 655-680, 1989.

Brocher, T. M., and N. I. Christensen, Seismic anisotropy due to preferred mineral orientation observed in shallow crustal rocks in southern Alaska, *Geology*, *18*, 737-740, 1990.

Center of Regional Geophysical and Geoecological Research (GEON), Russian Ministry of Geology, Atlas of seismic refraction profiles, Moscow, 1994.

Christensen, N. I., Compressional wave velocities in metamorphic rocks at pressures to 10 kbar, *J. Geophys. Res.*, *70*, 6147-6164, 1965.

Christensen, N. I., Compressional wave velocities in possible mantle rocks to pressures of 30 kbar, *J. Geophys. Res.*, *79*, 407-412, 1974.

Christensen, N. I., Compressional wave velocities in rocks at high temperatures and pressures, critical thermal gradients, and crustal low velocity zones, *J. Geophys. Res.*, *84*, 6849-6857, 1979.

Christensen, N. I., Seismic velocities, in *Handbook of Physical Properties of Rocks*, vol. 2, edited by R. S. Carmichael, pp. 1-228, CRC Press, Boca Raton, Fla., 1982.

Christensen, N. I., Measurements of dynamic properties of rock at elevated pressures and temperatures, in *Measurement of Rock Properties at Elevated Pressures and Temperatures*, edited by H. J. Pincus and E. R. Hoskins, pp. 93-107, American Society for Testing and Materials, Philadelphia, Pa., 1985.

Christensen, N. I., Reflectivity and seismic properties of the deep continental crust, *J. Geophys. Res.*, *94*, 17,793-17,804, 1989.

Christensen, N. I., and D. M. Fountain, Constitution of the lower continental crust based on experimental studies of seismic velocities in granulite, *Geol. Soc. Am. Bull.*, *86*, 227-236, 1975.

Christensen, N. I., and M. H. Salisbury, Structure and constitution of the lower oceanic crust, *Rev. Geophys.*, *13*, 57-86, 1975.

Christensen, N. I., and G. H. Shaw, Elasticity of mafic rocks from the Mid-Atlantic Ridge, *Geophys. J. R. Astron. Soc.*, *20*, 271-284, 1970.

Clarke, F. W., and H. S. Washington, The composition of the Earth's crust, *U.S. Geol. Surv. Prof. Pap.*, *127*, 117 pp., 1924.

Collins, C. D. N., Seismic velocities in the crust and upper mantle of Australia, *Rep. 277, Bur. Miner. Resour., Geol. and Geophys.*, Canberra, 159 pp., 1988.

Downs, H., The nature of the lower continental crust of Europe: Petrologic and geochemical evidence from xenoliths, *Phys. Earth Planet. Inter.*, *79*, 195-218, 1993.

Drummond, B. J., A review of crust/upper mantle structure in the Precambian areas of Australia and implications for Precambrian crustal evolution, *Precambrian Res.*, *40/41*, 101-116, 1988.

Durrheim, R. J., and W. D. Mooney, Archean and Proterozoic crustal evolution: evidence from crustal seismology, *Geology*, *19*, 606-609, 1991.

Durrheim, R. J., and W. D. Mooney, Archean and Proterozoic crustal evolution: Evidence from crustal seismology--Reply, *Geology*, *20*, 665-666, 1992.

Durrheim, R. J., and W. D. Mooney, Evolution of the Precambrian lithosphere: Seismological and geochemical constraints, *J. Geophys. Res.*, *99*, 15,359-15,374, 1994.

England, P. and G. Houseman, Extension during continental convergence with application to the Tibetan Plateau, *J. Geophys. Res.*, *94*, 15,561-15,569, 1989.

Fielitz, K., Elastic wave velocities in different rocks at high pressure and temperatures up to 750°C, *Z. Geophys.*, *20*, 943-956, 1971.

Fountain, D. M., and N. I. Christensen, Composition of the continental crust and upper mantle; A review, in Geophysical Framework of the Continental United States, edited by L. C. Pakiser and W. D. Mooney, *Mem. Geol. Soc. Am.*, *172*, 711-742, 1989.

Fountain, D. M., and M. H. Salisbury, Exposed cross sections through the continental crust; Implications for crustal structure, petrology, and evolution, *Earth Planet. Sci. Lett.*, *56*, 263-277, 1981.

Fowler, C. M. R., *The Solid Earth: An Introduction to Global Geophysics*, 472 pp., Cambridge University Press, New York, 1990.

Fuchs, K., and G. Muller, Computation of synthetic seismograms with the reflectivity method and comparison with observations, *Geophys. J.R. Astron. Soc.*, *23*, 417-433, 1971.

Garland, G. D., *Introduction to Geophysics: Mantle, Core and Crust*, 384 pp., W. B. Sanders, Philadelphia, Pa., 1979.

Giese, P., C. Prodehl, and A. Stein, *Explosion Seismology in Central Europe*, 429 pp., Springer-Verlag, New York, 1976.

Goodwin, A. M., *Precambrian Geology: The Dynamic Evolution of the Continental Crust*, 666 pp., Academic, San Diego, Calif., 1991.

Hamilton, W. B., and W. B. Meyers, Cenozoic tectonics of the western United States, *Rev. Geophys.*, *4*, 509-549, 1966.

Holbrook, W. S., W. D. Mooney, and N. I. Christensen, The seismic velocity structure of the deep continental crust, in *Lower Continental Crust*, edited by D. M. Fountain, R. Arculus and R. Kay, pp. 1-43, Elsevier, New York, 1992.

Hughes, D. S., and C. Maurette, Variation of elastic wave velocities in granites with pressure and temperature, *Geophysics*, *21*, 277,284, 1956.

James, D. E., and J. S. Steinhart, Structure beneath the continents: A critical review of explosion studies 1960-1965, in *The Earth Beneath the Continents, Geophys. Monogr. Ser.*, vol. 10, edited by J.S. Steinhart and T.J. Smith, pp. 293-333, AGU, Washington, D.C., 1966.

Kaila, K. L., and V. G. Krishna, Deep seismic sounding studies in India and major discoveries, in Seismology in India, An Overview, edited by H.K. Gupta, *Current Sci.*, *62*, 1992.

Kay, R. W., and S. M. Kay, The nature of the lower continental crust: Inferences from geophysics, surface geology and crustal xenoliths, *Rev. Geophys.*, *19*, 271-297, 1981.

Kay, R. W., and S. M. Kay, Creation and destruction of lower continental crust, *Geol. Rundsch.*, *80*, 1-20, 1991.

Kern, H., The effect of high temperature and high confining pressure on compressional wave velocities in quartz-bearing and quartz-free igneous and metamorphic rocks, *Tectonophysics*, *44*, 185-203, 1978.

Lachenbruch, A. H., and J. H. Sass, Heat flow and the thermal regime of the crust, in *The Earth's Crust: Its Nature and Physical Properties, Geophys. Monogr. Ser.*, vol. 20, edited by J. G. Heacock, pp. 626-675, AGU, Washington, D.C., 1977.

Li, S. L., and W. D. Mooney, Review of the crustal structure of China from seismic refraction profiling, *Tectonophysics*, in press, 1995.

McConnell, R. K., Jr., R. N. Gupta, and J. T. Wilson, Compilation of deep crustal seismic refraction profiles, *Rev. Geophys.*, *4*, 41-100, 1966.

McGetchin, T. R., and L. T. Silver, A crustal-upper mantle model for the Colorado Plateau based on observation of crystalline rock fragements in the Moses Rock Dike, *J. Geophys. Res.*, *77*, 7022-7057, 1972.

Mechie, J., and C. Prodehl, Crustal and uppermost mantle structure beneath the Afro-Arabian rift system, *Tectonophysics*, *153*, 103-121, 1988.

Mechie, J., G.R. Keller, C. Prodehl, S. Gaciri, L.W. Braile, W.D. Mooney, D. Gajewski, and K.J. Sandmeier, Crustal structure be-

neath the Kenya Rift from axial profile data, in *Crustal and Upper Mantle Structure of the Kenya Rift*, edited by G.R. Keller and M.A. Khan, *Tectonophysics, 236*, 179-200, 1994.

Meissner, R., *The Continental Crust; A Geophysical Approach*, 426 pp., Academic, San Diego, Calif., 1986.

Meissner, R., T. Wever, and E. R. Flueh, The Moho in Europe--Implications for crustal development, *Ann. Geophys., B5*, 357-364, 1987.

Meissner, R. O., and W. D. Mooney, Speculations on continental crustal evolution, *Eos Trans. AGU., 72*, 585, 590, 1991.

Miller, D. J., and N. I. Christensen, Seismic signature and geochemistry of an island arc: A multidisciplinary study of the Kohistan accreted terrane, northern Pakistan, *J. Geophys. Res., 99*, 11,623-11,642, 1994.

Mohorovicic, A., Das bebenvom 8, X, *Jahrb. Meterol. Obs. Zagreb, 9*, 1-63, 1909.

Mooney, W. D., Seismic methods for the determination of earthquake source parameters and lithospheric structure, in Geophysical Framework of the Continental United States, edited by L. C. Pakiser and W. D. Mooney, *Mem. Geol. Soc. Am., 172*, 11-34, 1989.

Mooney, W. D., and L. W. Braile, The seismic structure of the continental crust and upper mantle of North America, in *The Geology of North America - An Overview*, edited by A. W. Bally and A. R. Palmer, pp. 39-52, Geological Society of America, Boulder, Colo., 1989.

Morgan, P., and W. D. Gosnold, Heat flow and thermal regimes in the continental United States, in Geophysical Framework of the Continental United States, edited by L. C. Pakiser and W. D. Mooney, *Mem. Geol. Soc. Am., 172*, pp. 493-522, 1989.

Nafe, J. E., and C. L. Drake, Variation with depth in shallow and deep water marine sediments of porosity, density and the velocities of compressional and shear waves, *Geophysics, 22*, 523-552, 1957.

Nelson, K. D., A unified view of cratonic evolution motivated by recent deep seismic reflection and refraction results, *Geophys. J. Int., 105*, 25-35, 1991.

Pakiser, L. C., and R. Robinson, Composition and evolution of the continental crust as suggested by seismic observations, *Tectonophysics, 3*, 547-557, 1966.

Pavlenkova, N. I., Generalized geophysical model and dynamic properties of the continental crust, *Tectonophysics, 59*, 381-390, 1979.

Percival, J. A., D. M. Fountain, and M. H. Salisbury, Exposed crustal cross sections as windows on the lower crust, in *Continental Lower Crust*, edited by D.M. Fountain, R. Arculus and R.W. Kay, pp. 317-362, Elsevier, New York, 1992.

Plafker, G., W. J. Nokleberg, and J. S. Lull, Bedrock geology and tectonic evolution of the Wrangellia, Penninsular, and Chugach terranes along the Trans-Alaska Crustal Transect in the Chugach Mountains and southern Copper River Basin, Alaska, *J. Geophys. Res., 94*, 4255-4295, 1989.

Press, F., Seismic velocities, in Handbook of Physical Constants, edited by S. P. Clark Jr., *Mem. Geol. Soc. Am., 97*, 195-222, 1966.

Prodehl, C., Structure of the Earth's crust and upper mantle, *Landoldt Bornstein, 11A*, 97-206, 1984.

Raitt, R. W., G. G. Shor Jr., T. J. G. Francis, and G. B. Morris, Anisotropy of the Pacific upper mantle, *J. Geophys. Res., 74*, 3095-3109, 1969.

Ringwood, A. E., and D. H. Green, An experimental investigation of the gabbro-eclogite transformation and some geophysical implications, *Tectonophysics, 3*, 383-427, 1966.

Roy, R. F., E. R. Decker, D. D. Blackwell, and F. Brich, Heat flow in the United States, *J. Geophys. Res., 73*, 5207-5222, 1968.

Rudnick, R.L., Xenoliths--Samples of the lower continental crust, in *Lower Continental Crust*, edited by D.M. Fountain, R. Arculus and R. Kay, pp. 269-308, Elsevier, New York, 1992.

Schmidt, R., and B. J. Wood, Phase relationships in granulitic metapelites from the Ivrea-Verbano Zone (northern Italy), *Contrib. Mineral. Petrol., 54*, 225-279, 1976.

Smithson, S. B., R. A. Johnson, and Y. K Wong, Mean crustal velocity: a critical parameter for interpreting crustal structure and crustal growth, *Earth Planet. Sci. Lett., 53*, 323-332, 1981.

Soller, D. R., R. D. Ray, and R. D. Brown, A new global crustal thickness map, *Tectonics, 1*, 125-150, 1982.

Taylor, S. R., and S. M. McLennan, The composition and evolution of the continental crust; rare earth element evidence from sedimentary rocks, *Philos. Trans. R. Soc. London, A, 301*, 381-399, 1981.

Tuve, M. A., H. E. Tatel, and P. J. Hart, Crustal structure from seismic exploration, *J. Geophys. Res., 59*, 415-422, 1954.

Twiss, R. J., and E. M. Moores, *Structural Geology*, 532 pp., W. H. Freeman, New York, 1992.

Warren, D. H., and J. H. Healy, Structure of the crust in the conterminous United States, in *The Structure of the Earth's Crust, Dev. Geotecton.*, vol. 8, edited by St. Mueller, pp. 203-213, Elsevier, New York, 1974.

Weaver, B. L., and J. Tarney, Major and trace element composition of the continental lithosphere, in *Structure and Evolution of the Continental Lithosphere*, edited by H. N. Pollack and V. R. Murthy, pp. 39-68, Pergamon, New York, 1984.

Windley, B. F., *The Evolving Continents*, 399 pp., John Wiley, New York, 1984.

Woollard, G. P., Crustal structure from gravity and seismic measurements, *J. Geophys. Res., 64*, 1521-1544, 1959.

N. I. Christensen, Department of Earth and Atmospheric Sciences, Purdue University, West Lafayette, IN 47907-1397. (e-mail: chris@geo.purdue.edu)

W. D. Mooney, U. S. Geological Survey, 345 Middlefield Road, MS 977, Menlo Park, CA 94025. (e-mail: mooney@ andreas.wr.usgs.gov)

(Received August 30, 1994; revised January 19, 1995;
accepted January 23, 1995.)